

Design of a Power System Stabilizer Using Adaptive Neuro-Fuzzy Logic

by

(Moudud Ahmed)

A thesis submitted in partial fulfillment of the requirements for the degree
of Master of Science in Electrical and Electronic Engineering



Khulna University of Engineering & Technology

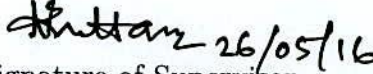
Khulna 9203, Bangladesh


May 2016

Dedicated to My Parents

Declaration

This is to certify that the thesis work entitled "Design of a Power System Stabilizer Using Adaptive Neuro-Fuzzy Logic" has been carried out by Moudud Ahmed in the Department of Electrical and Electronic Engineering, Khulna University of Engineering & Technology, Khulna, Bangladesh. The above thesis work or any part of this work has not been submitted anywhere for the award of any degree or diploma.

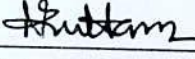
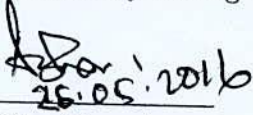
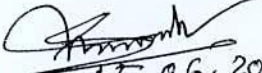



Signature of Supervisor


Signature of Candidate

Approval

This is to certify that the thesis work submitted by Moudud Ahmed entitled "Design of a Power System Stabilizer Using Adaptive Neuro-Fuzzy Logic" has been approved by the board of examiners for the partial fulfillment of the requirements for the degree of Master of Science in Electrical and Electronic Engineering from the Department of Electrical and Electronic Engineering, Khulna University of Engineering & Technology, Khulna, Bangladesh in May 2016.

BOARD OF EXAMINERS

1.  26/5/2016
Dr. Naruttam Kumar Roy
Assistant Professor
Department of Electrical and Electronic Engineering
Khulna University of Engineering & Technology
Chairman
(Supervisor)
2.  26.05.2016
Head of the Department
Department of Electrical and Electronic Engineering
Khulna University of Engineering & Technology
Member
3.  15.06.2016
Dr. Bashudeb Chandra Ghosh
Professor, Department of Electrical and Electronic Engineering
Khulna University of Engineering & Technology
Member
4.  26.05.2016
Dr. Md. Rafiqul Islam
Professor, Department of Electrical and Electronic Engineering
Khulna University of Engineering & Technology
Member
5.  26/05/2016
Dr. Md. Rafiqul Islam Sheik
Professor, Department of Electrical and Electronic Engineering
Rajshahi University of Engineering & Technology
Member
(External)

Abstract

Power systems are large, complex and nonlinear systems, and often exhibit low-frequency power oscillations due to insufficient damping. PSSs are widely used to suppress the electromechanical oscillations of generators and thus, enhance the overall stability of power systems. The conventional PSS which uses lead-lag compensation and gain settings for particular operating conditions provides poor performance under different loading conditions. To mitigate the shortcomings of conventional PSS, Artificial Intelligence (AI) based techniques such as Fuzzy Logic Controller (FLC) and Adaptive Neuro-Fuzzy Inference System (ANFIS) have been introduced. FLC based PSS does not require mathematical model, possess lesser computational time, and ensures good performance under all conditions. However, speed and robustness are the most significant properties in comparison to the other classical schemes, there are no practical systematic procedures for the FLPSS design, so the rules and the membership functions of the controller are tuned subjectively, making the design laborious and a time-consuming task. On the other hand, an ANFIS based technique is a promising method, which adjusts membership functions and rules adaptively to improve a systems performance. In literature, ANFIS-PSS is implemented for multi-machine power system having constant impedance load. The main contribution of this thesis is to introduce a PSS for a multi-machine interconnected power system comprising a dynamic load grounded on adaptive-neuro fuzzy logic technique. Load dynamics is included because it has significant impact on power system dynamic analysis. Transient stability analysis is more concerned with dynamic behaviors of loads. The robustness of ANFIS-PSS is being tested by applying single line to ground

faults and symmetrical three phase faults. Another contribution of this thesis is to analyze the performance of using various input signals to PSS. It is found that the performance of an ANFIS-PSS depends on the input signal to PSS and for speed deviation and accelerating power as an input signal, the performance is quite far better compared to the selection of other inputs utilized in this work.

Acknowledgment

In this very special moment, first and foremost I would like to express my heartiest gratitude to the almighty God for allowing me to accomplish my research successfully. I am really thankful for the enormous blessings that the Almighty has bestowed upon me not only during my study period but also throughout my life.

My utmost gratitude to my supervisor Dr. Naruttam Kumar Roy, Assistant Professor, Department of Electrical and Electronic Engineering, Khulna University of Engineering and Technology for his constant motivation, support, expert guidance, useful comments, which enabled me to enrich my knowledge and reach the final destination.

I extend my sincere gratitude and appreciation to Dr. Md. Rafiqul Islam (2), Dr. Mohammad Saifur Rahman , Dr. M. A. Samad, Dr. Md. Abdur Rafiq, Dr. Mostafa Zaman Chowdhury who had been my course teachers during my graduate studies. I would also like to thank my faculty colleagues in Bangabandhu Sheikh Mujibur Rahman Science and Technology University, Gopalganj for their kind cooperation and providing me an excellent work environment during the MSc program. Lastly, I offer my regards and blessings to all of those who supported me in any respect during the completion of the thesis.

Moudud Ahmed

Table of Contents

Acknowledgment	i
Abstract	ii
List of Figures	vii
List of Tables	x
Chapter 1 Introduction	1
1.1 Background	1
1.2 Motivation	2
1.3 Literature Review	3
1.4 Objectives	6
1.5 Organization of this Thesis	6
Chapter 2 System Model	8
2.1 Introduction	8
2.2 Power System Stability	8
2.2.1 Rotor Angle Stability	9
2.2.2 Voltage Stability	11
2.2.3 Frequency Stability	12
2.3 Synchronous Generator Model	13
2.4 Matlab/Simulink Dialog Box and Parameters	14
2.4.1 Rotor Type	16
2.4.2 Nominal Power, Voltage, and Frequency	16
2.4.3 Reactances	16

2.4.4	Time Constants (d-axis and q-axis)	16
2.4.5	Time Constants	16
2.4.5.1	Stator Resistance	16
2.4.6	Inertia, Friction Factor, and Pole Pairs	16
2.4.7	Initial Conditions	17
2.5	Power System Stabilizer Model	17
2.6	Dynamic Load	18
2.6.1	Exponential Dynamic Load Model	20
2.7	Load Flow and Machine Initialization	20
2.8	Conclusion	22
Chapter 3 Conventional Power System Stabilizers		23
3.1	Introduction	23
3.2	Heffron-Phillips Model of Single Machine Infinite Bus System	24
3.3	Proportional Integral Derivative (PID) Controller based AVR	25
3.4	Root Locus Design	26
3.4.1	Design of AVR	26
3.4.2	PSS Design using Root Locus	26
3.5	Frequency Response Design	26
3.5.1	Design of AVR	28
3.5.2	Design of PSS	29
3.6	PSS Design using Artificial Intelligence	32
3.6.1	FLPSS Design	32
3.6.2	ANFIS based PSS Design	33
3.7	Simulation Results	34
3.8	Conclusion	35
Chapter 4 Design of a PSS Using ANFIS for a Multi-Machine System Having Dynamic Loads		36
4.1	Introduction	36

4.2	Fuzzy Logic Controller	36
4.3	Fuzzy Sets	38
4.4	Membership Functions	38
4.5	Implication Methods	39
4.6	Controller Design Precedure	39
4.7	Fuzzy PSS Design in Mamdani Form	40
4.8	Artificial Neural Networks	40
4.9	Training Procedure for ANFIS Network	44
4.10	Hybrid Learning Algorithm	45
4.11	Adaptive-Neuro Fuzzy Controller	46
4.12	Problem Description	46
4.13	Simulation Results	49
4.14	Conclusion	53
Chapter 5 Selection of Best Input Signal for ANFIS-PSS		54
5.1	Introduction	54
5.2	Selection of best input signal	54
5.3	Simulation Results	54
5.4	Conclusion	61
Chapter 6 Conclusions and Future Work		62
6.1	Conclusion	62
6.2	Future Research Directions	62
Bibliography		63
A		68

List of Figures

2.1	The overall picture of the stability problem	9
2.2	Matlab block of synchronous machine	13
2.3	Block parameters of synchronous machine	15
2.4	Thyristor excitation system with AVR and PSS	18
2.5	Three phase dynamic load block	19
2.6	Load flow and machine initialization block	21
3.1	Block diagram of SMIB system.	24
3.2	Simulink structure of SMIB with PID as AVR.	25
3.3	Step response for 0.1pu step input and different values of K_i	27
3.4	Uncompensated system root locus.	27
3.5	Final compensated system root locus plot.	28
3.6	Frequency response plot with and without VR loop.	29
3.7	Step response of lag compensator as voltage regulator for 0.1pu step input.	30
3.8	Separation of speed control loop.	31
3.9	Frequency response of damping loop.	31
3.10	Root locus of PSS loop with compensator.	32
3.11	Matlab/Simulink model of SMIB with fuzzy logic controller.	33
3.12	Response of rotor angle for a 5% change in mechanical input.	34
3.13	Response of rotor speed deviation for a 5% change in mechanical input.	35

4.1	FLC structure	37
4.2	Input MF ($\Delta\omega_r$)	41
4.3	Input MF ($\Delta\dot{\omega}_r$)	42
4.4	Output MF (ΔV_{PSS})	42
4.5	The architecture of the ANFIS.	44
4.6	Triangular fuzzy MF	45
4.7	ANFIS-PSS design procedure	47
4.8	Training error of ANFIS	48
4.9	Architecture of T-S type ANFIS controller	48
4.10	Two area network with a dynamic load	49
4.11	The terminal voltage characteristics of generator 1 and generator 3 for static loads.	50
4.12	The terminal voltage characteristics of generator 1 and generator 3 for dynamic loads.	50
4.13	Comparative analysis of rotor speed deviation of G2 at A-1 for FLPSS and ANFIS-PSS (symmetrical three-phase fault).	51
4.14	Comparative performance of terminal voltage (vt) of G1 and G3 for FLPSS and ANFIS-PSS (symmetrical three-phase fault).	52
4.15	Active power flow from A-1 to A-2 for FLPSS and ANFIS PSS (symmetrical three-phase fault).	52
4.16	Voltage across dynamic load terminal (bus 7) for FLPSS and ANFIS-PSS (symmetrical three-phase fault).	53
5.1	Matlab simulink model of two area test system.	55
5.2	Simulink model of two area test system with ANFIS-PSS for speed deviation and voltage as input to PSS.	56
5.3	Simulink model of two area test system with ANFIS-PSS for speed deviation and angular acceleration as input to PSS.	56

5.4	Simulink model of two area test system with ANFIS-PSS for speed deviation and accelerating power as input to PSS.	57
5.5	Comparative analysis of rotor speed deviation of G 3 at A-2 (single line to ground fault).	57
5.6	Comparative analysis of active power flow from A-1 to A-2 (single line to ground fault).	58
5.7	Comparative analysis of terminal voltage(vt) of G 2 at A-1 (single line to ground fault).	58
5.8	Comparative performance of terminal voltage (vt) of G2 at A-1 (three phase to ground fault).	59
5.9	Comparative analysis of rotor speed deviation of G 3 at A-2 (three phase to ground fault).	59
5.10	Comparative analysis of active power flow from A1 to A2 (three phase to ground fault).	60

List of Tables

4.1	Linguistic Variables of FLC	40
4.2	Rule Table of FLC	41

1.1 Background

The power system is a dynamic system. It is continuously being subjected to disturbances, which cause the generator voltage and rotor angle to change. When these disturbances die out, a new acceptable steady state operating condition is reached. It is important that these disturbances do not drive the system to unstable condition. The disturbances may be of local mode having frequency range of 0.7 to 2 Hz or of inter area modes having frequency range in 0.1 to 0.8 Hz, these swing are due to the poor damping characteristics caused by modern voltage regulators with high gain [1,2]. A high gain regulator through excitation control has an important effect of eliminating synchronizing torque it affects the damping torque negatively. To compensate the unwanted effect of these voltage regulators, additional signals are introduced in feedback loop of voltage regulators. The additional signals are mostly derived from speed deviation or accelerating power. This is achieved by injecting a stabilizing signal into the excitation system voltage reference summing point junction. The device setup to provide this signal is called power system stabilizer. Excitation control is well known as one of the effective means to enhance the overall stability of electrical power systems. Present day excitation systems predominantly constitute the fast acting AVR's. A high response exciter is beneficial in increasing the synchronizing torque, thus enhancing the transient stability i. e. to hold the generator in synchronism with power system during large transient fault condition. However, it provides a negative damping especially at high values of external system reactance and high

generator outputs.

1.2 Motivation

Operating conditions of a power system are continually changing due to load level, generation variations, and line switching. Such changes can induce transient low-frequency oscillations, which are difficult to control. A convenient yet effective way of damping these oscillations is through the use of power system stabilizers (PSSs), which produce positive damping signals to cancel out negative damping of the excitation system introduced under some fault or other operating conditions. A classical lag-lead PSS can be optimized to work under some narrow range of operating conditions. However, its damping performance deteriorates as conditions change or when network switching takes place. So typically, an adaptive mechanism is used to tune the PSS parameters according to the new operating point. By contrast, a fuzzy inference system employing fuzzy if-then rules can model the qualitative aspects of human knowledge and reasoning processes without employing precise quantitative analyses. This fuzzy modeling or fuzzy identification, first explored systematically by Takagi and Sugeno [3], has found numerous practical applications in control [4], prediction and inference [5]. However, there are some basic aspects of this approach which are in need of better understanding. More specifically, firstly no standard methods exist for transforming human knowledge or experience into the rule base and database of a fuzzy inference system, and secondly there is a need for effective methods for tuning the membership functions (MFs) so as to minimize the output error measure or maximize performance index. In this perspective, the aim of this research is to suggest a novel architecture called Adaptive-Network-based Fuzzy Inference System, or simply ANFIS, which can serve as a basis for constructing a set of fuzzy if-then rules with appropriate membership functions to generate the stipulated input-output pairs.

1.3 Literature Review

A well-regulated power system is expected to supply consumers with uninterrupted, sufficient and reliable power at least cost [6]. To achieve and maintain this reliability, the power system must be stable and secure [6, 7]. Power systems are inherently nonlinear and undergo a wide range of transient conditions. Large-scale power systems are composed of control areas or regions representing coherent groups of generators. These areas are interconnected through tie lines. The tie lines are utilized for energy exchange between areas and provide inter-area support in case of abnormal condition. Stressed operating conditions can increase the possibility of inter-area oscillations between different control areas and can even lead to the breakup of the whole system [7, 8]. Electromechanical oscillations can be classified in two main categories (i) Local Plant Mode Oscillations and, (ii) Inter-area Oscillations. The former type is associated with units at a generating station swinging with respect to the rest of the power system. Such oscillations are referred to as local plant mode oscillations. The frequencies of these oscillations are typically in the range 0.8Hz to 2.0 Hz. The second type of oscillation is associated with the swinging of many machines in one part of the system against machines in other parts. These are referred to as inter area mode oscillations and have frequencies in the range 0.1 to 0.7 Hz. The oscillations of small signal magnitude with low frequency due to insufficient damping caused by adverse operating conditions often persist for long period of time and sometimes may hinder power transfer capability with reduced security level [2]. In the late 1950s and early 1960s most of the new generating units added to electric utility systems were equipped with continuously acting voltage regulators [9]. The generator excitation system maintains generator voltage and controls the reactive power flow using an automatic voltage regulator (AVR). The role of an AVR is to hold the terminal voltage magnitude of a synchronous generator at a specified level [10]. The AVR is so designed as to be able to respond quickly to a dis-

turbance endangering the transient stability [11, 12]. Also, it should be able to contribute in improving the small signal stability of the system. But, the conventional AVR is a fixed gain device. The gain is intentionally made high to ensure fast response. But, high gain of AVR circuit often becomes detrimental from the point of view of small signal stability. So, a compromise is to be done [13, 14]. In order to mitigate these problems, Power System Stabilizers (PSS) are used in conjunction with AVRs. The action of PSS is to extend angular stability limits of a power system by providing supplemental damping to the rotor models oscillations through generator excitation. This damping is provided by an electric torque applied to the rotor is in phase with the speed variation [15].

PSSs were developed to aid in damping these oscillations via modulation of the generator excitation. The art and science of applying power system stabilizers (PSS) has been developed over the past 40 to 45 years since the first widespread application to the Western systems of the United States [9]. Conventional PSS (CPSS) is widely used in existing power systems and has made a contribution in enhancing power system dynamic stability. The parameters of CPSS are determined based on a linearized model of the power system and, around a nominal operating point where they are designed can provide good performance. As loads play an important role in power system stability study, the incorporation of load dynamics during a PSS design is essential. Moreover, the induction motor loads which are considered as dynamic loads, account for a large portion of electric loads, especially in large industries and air-conditioning in the commercial and residential areas. the topic of load modeling occupies a large volume in power systems literature. The dynamic behavior of loads may lead to inconsistent results for dynamic stability and voltage collapse studies [15–21]. Since power systems are highly non-linear systems, with configurations and parameters that change with time, the CPSS design based on the linearized model of the power system cannot guarantee its performance in a practical operating environment [22, 23].

To solve these problems, Artificial Intelligence (AI) is widely used. Among

various AI techniques, fuzzy logic control appears to be the most promising, due to its lower computational burden and robustness. Also, a mathematical model is not required to describe the system in fuzzy logic based PSS (FLPSS) design. But, the main problem with the conventional fuzzy controllers is that the parameters associated with the membership functions and the rules depend broadly on the intuition of the engineers. If it is required to change the parameters, it is to be done by trial and error only. There is no scientific optimization methodology inbuilt in the general fuzzy inference system [13]. To overcome this limitation, Adaptive Neuro-Fuzzy Inference System (ANFIS) is used. In ANFIS, rather than choosing the parameters associated with a given membership function arbitrarily, these parameters are chosen so as to tailor the membership functions to the input/output data in order to account for these types of variations in the data values. This action of learning method works in the same manner as neural networks [13, 24].

There is a rich literature on the PSS design using Adaptive Neuro-Fuzzy Inference System (ANFIS) having constant impedance loads [25–27]. It is observed that ANFIS controller is found to be more suitable than Fuzzy Logic PSS in present day power system where complexity is gradually increasing day by day. As loads play an important role in power system stability study, the incorporation of load dynamics during a PSS design is essential [28, 29]. Transient stability analysis is more concerned with dynamic behaviors of loads. However, the performance of ANFIS based PSS solely depends on the proper selection of input signals. The issue related to the selection of input to PSS is not adequately covered in the available literature. Therefore, to find the best input for the proposed controller is one of the prime concerns of this research.

1.4 Objectives

Whenever a disturbance occurs in the system like generation/load imbalance or any fault, the system may lose its stability or cause poorly damped oscillations. To improve the performance of system, the objectives of the proposed research are as follows:

- Determining the stability of power system using eigenvalue analysis.
- Utilizing step by step mathematical model of a single machine infinite bus (SMIB) system for stability analysis.
- Designing a power system stabilizer (PSS) using conventional methods (Root Locus method, Frequency Response method) for SMIB system and comparing the performance of the above mentioned conventional PSSs.
- Designing a Fuzzy logic controller for damping oscillations of test systems having dynamic loads.
- Optimizing the parameters of Fuzzy logic PSS using Adaptive Neuro Fuzzy Inference System (ANFIS).
- Selection of the best input signal for ANFIS based PSS and examining its robustness.

1.5 Organization of this Thesis

The dissertation is organized as follows:

- **Chapter I Introduction.** Covers literature review of power system stabilizers and general introduction of the thesis.
- **Chapter II System Model.** Presents the power system model, dynamic load model, and formation of power system in Matlab/Simulink environment.

- **Chapter III Conventional Power System Stabilizer Design.** Presents different approaches for the design of a conventional power system stabilizer (CPSS) and compares their performances.
- **Chapter IV Design of a PSS Using ANFIS for a Multi-Machine System Having Dynamic Loads.** The fuzzy logic and ANFIS design techniques are described. The effectiveness of the proposed method is also verified here.
- **Chapter V Input Signal Selection For ANFIS Based PSS.** Presents brief discussion on input signal selection for ANFIS-PSS design method.
- **Chapter VI Conclusion and the Future Work.** Brings a conclusion and suggestions for the future work.

2.1 Introduction

For small signal stability analysis, the detail mathematical model that describing the power system are needed. Small signal analysis using linear techniques provides valuable information about the inherent dynamic characteristics of the power system and assists in its design. This chapter reviews a general introduction to the power system stability problem, basic concepts, classification, definitions of related terms, and analytical techniques useful in the study of small signal stability.

2.2 Power System Stability

Power system stability has been recognized as an important problem for secure system operation since the 1920s [6, 30]. The definition of power system stability is the ability of power system to reach a state of equilibrium after being subjected to a disturbance. When subjected to a disturbance, the power system stability depends on the initial condition of the system and the nature of the system. Large power system stability phenomena are commonly classified as

- Rotor Angle Stability
- Voltage Stability
- Frequency Stability

The figure 2.1 shows the overall picture of the stability problem

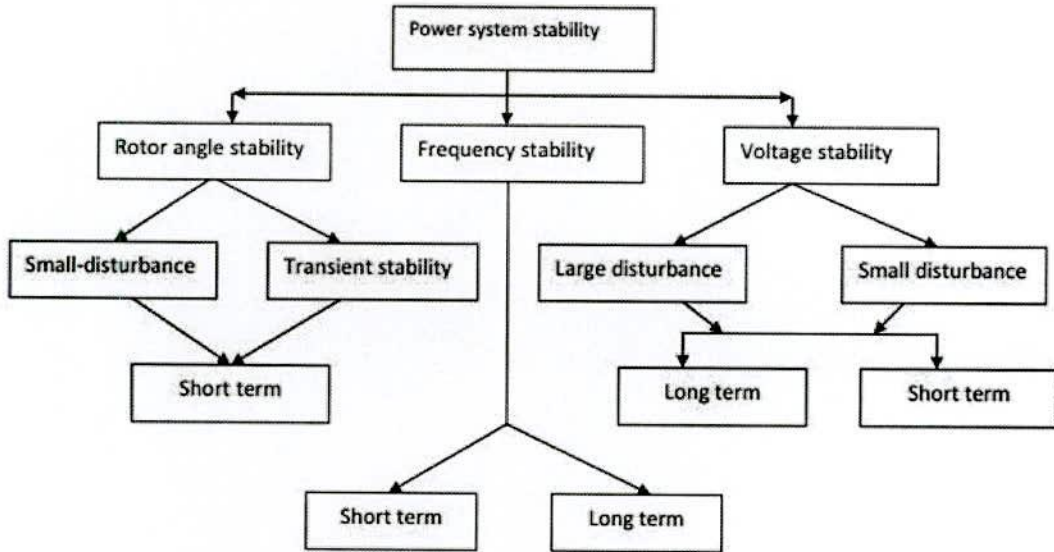


Figure 2.1: The overall picture of the stability problem

2.2.1 Rotor Angle Stability

This refers to the ability of the synchronous generator in an interconnected power system to remain in synchronism after being subjected to disturbances. It depends on the ability of the machine to maintain equilibrium between electromagnetic torque and mechanical torque of each synchronous machine in the system [6]. Instability of this kind occurs in the form of swings of the generator rotor which leads to loss of synchronism. Under steady-state conditions, there is equilibrium between the input mechanical torque and the output electromagnetic torque of each generator, and the speed remains constant. If the system is perturbed, this equilibrium is destroyed. With the electric power systems, the change in electric torque of a synchronous machine following a perturbation can be resolved into two components:

$$\Delta T_e = T_s \Delta \delta + T_d \Delta \omega \quad (2.1)$$

Where, $T_s \Delta \delta$ is synchronizing torque component, in phase with rotor angle deviation, and T_s is the synchronizing torque coefficient.

$T_d\Delta\omega$ is damping torque component, in phase with the speed deviation, and T_d is damping torque coefficient.

System stability depends on the existence of both components of torque for each of the synchronous machines. Lack of sufficient synchronizing torque results in aperiodic or non-oscillatory instability, whereas lack of damping torque results in oscillatory instability. For convenience in analysis of the nature of stability problems, it is useful to characterize rotor angle stability in terms of the following two subcategories:

1. Small Disturbance Rotor Angle Stability
2. Large Disturbance Rotor Angle Stability

Small disturbance rotor angle stability is concerned with the ability of the power system to maintain a steady state operating point when subjected to small disturbances, e. g. small change in load. Small disturbance rotor angle stability is usually associated with insufficient damping. The time frame of interest in small disturbance stability studies is on the order of 10 to 20 seconds following a disturbance. Large disturbance rotor angle stability is associated with the ability of the power system or a small machine to maintain synchronism when subjected to a large disturbance in the power system, e.g. a fault on a transmission line, a short circuit, or a generator trip. Large disturbance rotor angle stability is associated with insufficient synchronizing torque. The time frame of interest in transient stability studies is usually 3 to 5 seconds following the disturbance. It may extend to 10 seconds for very large systems with dominant inter-area swings. The issue of small signal instability in current scenario is generally because of insufficient damping of oscillations. In practical power system, the main types of oscillations associated with small signal stability are as follows:

- Swing Mode
- Inter-area mode

- Control Mode
- Torsional Mode

Small-disturbance rotor angle stability problems may be either local or global in nature. Local problems involve a small part of the power system, and are usually associated with rotor angle oscillations of a single power plant against the rest of the power system. Such oscillations are called local plant mode oscillations. Stability (damping) of these oscillations depends on the strength of the transmission system as seen by the power plant, generator excitation control systems and plant output [1].

Global problems are caused by interactions among large groups of generators and have widespread effects. They involve oscillations of a group of generators in one area swinging against a group of generators in another area. Such oscillations are called inter-area mode oscillations.

Control modes are associated with generating units and other controls. Poorly tuned exciters, speed governors, HVDC converters and static var compensators are the usual causes of instability of these modes.

Torsional Modes are associated with the turbine generator shaft system rotational components. The instability of torsional modes may be caused by interaction with excitation controls, speed governors, HVDC controls and series capacitor compensated lines.

2.2.2 Voltage Stability

Voltage stability refers to the ability of a power system to maintain steady voltages at all buses in the system after being subjected to a disturbance from a given initial operating condition. It depends on the ability to maintain or restore equilibrium between load demand and load supply from the power system. Instability that may result occurs in the form of a progressive fall or rise of voltages of some buses. A possible outcome of voltage instability is loss of load in an area,

or tripping of transmission lines and other elements by their protective systems leading to cascading outages. Loss of synchronism of some generators may result from these outages or from operating conditions that violate field current limit [31]. The time frame of interest for voltage stability problems may vary from a few seconds to tens of minutes. Therefore, voltage stability may be either a short-term or a long-term phenomenon.

- Short-term Voltage Stability.
- Long-term Voltage Stability.

Short-term voltage stability involves dynamics of fast acting load components such as induction motors, electronically controlled loads, and HVDC converters. The study period of interest is in the order of several seconds and, analysis requires solution of appropriate system differential equations.

Long-term voltage stability involves slower acting equipment such as tap-changing transformers, thermostatically controlled loads, and generator current limiters. The study period of interest may extend to several or many minutes, and long-term simulations are required for analysis of system dynamic performance [32, 33].

2.2.3 Frequency Stability

Frequency stability refers to the ability of a power system to maintain steady frequency following a severe system upset resulting in a significant imbalance between generation and load. It depends on the ability to maintain or restore equilibrium between system generation and load, with minimum unintentional loss of load. Instability that may result occurs in the form of sustained frequency swings leading to tripping of generating units and or loads.

2.3 Synchronous Generator Model

The dynamics of a three-phase round-rotor or salient-pole synchronous machine is very much important in power system stability analysis. The block of synchronous machine in Matlab/Simulink is shown in Figure 2.2. The synchronous machine block can be operated either in generator or motor modes. The operating mode is determined by the sign of the mechanical power (positive for generator mode, negative for motor mode). The electrical part of the machine is represented by a sixth-order state-space model and the mechanical part is the same as in the Simplified Synchronous Machine block. The model takes into account the dynamics of the stator, field, and damper windings. The equivalent circuit of the model is represented in the rotor reference frame (q and d frame). All rotor parameters and electrical quantities are viewed from the stator [34].

The differential equations for the sixth order synchronous generator model

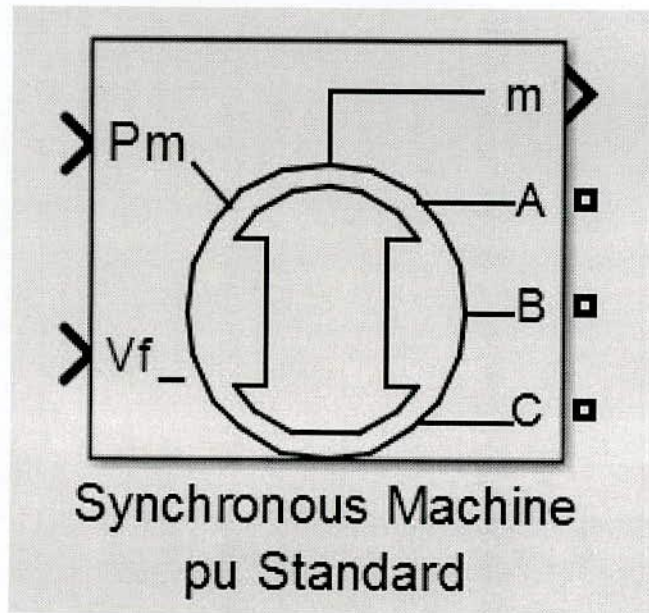


Figure 2.2: Matlab block of synchronous machine

including leakage reactance are given by equation (2.2) to equation (2.7) with notation consistent with [35].

$$\frac{d}{dt}E'_d = \frac{1}{T'_{qo}} \left[-E'_d + (X_q - X'_q) \left(I_q - \frac{X'_q - X''_q}{(X'_q - X_{lk,s})^2} (\Psi_{2q} + (X'_q - X_{lk,s})I_q + E'_d) \right) \right] \quad (2.2)$$

$$\frac{d}{dt} E'_q = \frac{1}{T'_{do}} \left[-E'_q - (X_d - X'_d) \left(I_d - \frac{X'_d - X''_d}{(X'_d - X_{lk,s})^2} (\Psi_{1d} + (X'_d - X_{lk,s}) I_d - E'_q) \right) + E_{fd} \right] \quad (2.3)$$

$$\frac{d}{dt} \Psi_{1d} = \frac{1}{T'_{do}} [-\Psi_{1d} + E'_q - (X'_d - X_{lk,s}) I_d] \quad (2.4)$$

$$\frac{d}{dt} \Psi_{2q} = \frac{1}{T'_{qo}} [-\Psi_{2q} - E'_d - (X'_q - X_{lk,s}) I_q] \quad (2.5)$$

$$\frac{d}{dt} \Delta\omega_r = \frac{1}{2H} [P_m - P_e - D\Delta\omega_r] \quad (2.6)$$

$$\frac{d}{dt} \delta = (\omega_r - \omega_s) = \Delta\omega_r \quad (2.7)$$

$$E_d = \frac{X''_q - X_{lk,s}}{X'_q - X_{lk,s}} E'_d - \frac{X'_q - X''_q}{X'_q - X_{lk,s}} \Psi_{2q} + X''_q I_q \quad (2.8)$$

$$E_q = \frac{X''_d - X_{lk,s}}{X'_d - X_{lk,s}} E'_q + \frac{X'_d - X''_d}{X'_d - X_{lk,s}} \Psi_{1d} + X''_d I_d \quad (2.9)$$

$$E_t = \sqrt{E_d^2 + E_q^2} \quad (2.10)$$

$$P_e = E_d I_d + E_q I_q \quad (2.11)$$

Where,

E_{dq} = Transient voltage in d-/q-axis

E_{fd} = Field Voltage

H = Inertia constant

I_{dq} = Current in d-/q-axis

$T_{do,qo}$ Transient time constant of d- /q-axis , $T'_{do,qo}$ Subtransient time constant of d-/q-axis

X'_{dq} Transient reactance in d- /q-axis

X''_{dq} = Subtransient reactance in d-/q-axis

X_{ls} Leakage reactance

δ = Rotor angle

ψ_{1d} Flux linkage d-axis damper winding

ψ_{2q} = Flux linkage q-axis damper winding

ω_r = Rotor speed

ω_s = Synchronous rotor speed

2.4 Matlab/Simulink Dialog Box and Parameters

In figure 2.3 shows the Block parameters of synchronous machine. In the power library there are three Synchronous Machine blocks to specify the parameters of the model. Brief description of each components are given bellow.

Block Parameters: M1 900 MVA

Configuration Parameters Advanced Load Flow

Nominal power, line-to-line voltage, frequency [Pn(VA) Vn(Vrms) fn(Hz)]
 [900E6 20000 60]

Reactances [Xd Xd' Xd'' Xq Xq' Xq'' Xl] (pu):
 [1.8 .3 .25 1.7 .55 .25 .2]

d axis time constants: Open-circuit

q axis time constants: Open-circuit

Time constants [Tdo' Tdo'' Tqo' Tqo''] (s):
 [8 .03 .4 .05]

Stator resistance Rs (pu):
 0.0025

Inertia coefficient, friction factor, pole pairs [H(s) F(pu) p()]:
 [6.5 0 4]

Initial conditions [dw(%) th(deg) ia,ib,ic(pu) pha,phb,phc(deg) Vf(pu)]:
 -32.1008 0.786531 0.786531 0.786531 1.59598 -118.404 121.596 1.85138

Simulate saturation

OK Cancel Help Apply

Figure 2.3: Block parameters of synchronous machine

2.4.1 Rotor Type

First, specify rotor type. It is Salient-pole or Round(cylindrical). This choice affects the number of rotor circuits in the q-axis (damper windings).

2.4.2 Nominal Power, Voltage, and Frequency

The total three-phase apparent power P_n (VA), RMS line-to-line voltage V_n (Vrms), frequency f_n (Hz). Since rotor quantities are viewed from the stator, they are converted to pu using the stator base quantities derived from the preceding three nominal parameters.

2.4.3 Reactances

The d-axis synchronous reactance X_d , transient reactance X'_d , and subtransient reactance X''_d , the q-axis synchronous reactance X_q , transient reactance X'_q (only if round rotor), and subtransient reactance X''_q , and finally the leakage reactance X_l . All the above mentioned values are in pu.

2.4.4 Time Constants (d-axis and q-axis)

Specify the time constants for each axis, either open-circuit or short-circuit, which is shown in figure 2.3.

2.4.5 Time Constants

The d-axis and q-axis time constants (all in s). These values must be consistent with choices made on the two previous lines: d-axis transient open-circuit (T'_{do}) or short-circuit (T'_d) time constant, d-axis subtransient open-circuit (T''_{do}) or short-circuit (T''_d) time constant, q-axis transient open-circuit (T'_{qo}) or short-circuit (T'_q) time constant (only if round rotor), q-axis subtransient open-circuit (T''_{qo}) or short-circuit (T''_q) time constant.

2.4.5.1 Stator Resistance

The stator resistance R_s (p.u.)

2.4.6 Inertia, Friction Factor, and Pole Pairs

The inertia coefficient J (kg.m²), damping coefficient D (N.m.s./rad), and number of pole pairs p .

2.4.7 Initial Conditions

The initial speed deviation $\Delta\omega$ (% of nominal speed), electrical angle of the rotor θ_e (degrees), line current magnitudes i_a, i_b, i_c (A) and phase angles pha, phb, phc (degrees), and the initial field voltage V_f (V). The initial field voltage can be specified in one of two ways. If the nominal field current is known (first line, last parameter), enter in the dialog box the initial field voltage in volts DC referred to the rotor. Otherwise, enter a zero as nominal field current, as explained earlier, and specify the initial field voltage in volts DC referred to the stator. The nominal field voltage can be viewed from the stator by selecting the display V_{fd} which produces a nominal V_t check box at the bottom of the dialog box.

2.5 Power System Stabilizer Model

The basic function of a power system stabilizer is to add damping to the generator rotor oscillations by controlling its excitation using auxiliary stabilizing signals. To provide damping, the stabilizer must produce a component of electrical torque in phase with the rotor speed deviations. PSS may not be required under normal operating conditions; they allow satisfactory operation under unusual or abnormal conditions which may be encountered at times. Thus, PSS has become a standard option with modern static exciters and it is essential for power engineers to use these effectively. Since the purpose of a PSS is to introduce a damping torque component, a logical signal to use for controlling generator excitation is the speed deviation ($\Delta\omega_r$). The PSS transfer function $G_{pss}(s)$ should have appropriate phase compensation circuit to provide phase lag between electrical torque and exciter input. The excitation system, including the AVR and PSS is shown in figure 2.4. The amount of damping is determined by the stabilizer gain K_{STAB} . The signal washout block serves as a high pass filter, with the time constant T_w high enough to allow signals associated with oscillations in ω_r to pass unaltered. In absence of washout block, small change in speed would modify the terminal voltage. The time constant T_w is not critical and may be in the range of 10 to 20 seconds. The main consideration is that it be long enough to pass stabilizing signals at the frequencies of interest unchanged, but not so long that it leads to undesirable generator voltage excursions during system islanding conditions. The phase compensation block provides the appropriate phase lead characteristic to compensate for the phase lag between the exciter input and the generator electrical (air-gap) torque. Normally, the frequency range of interest is 0.1 to 2.0 Hz and the phase lead network should provide compensation over this entire frequency range.

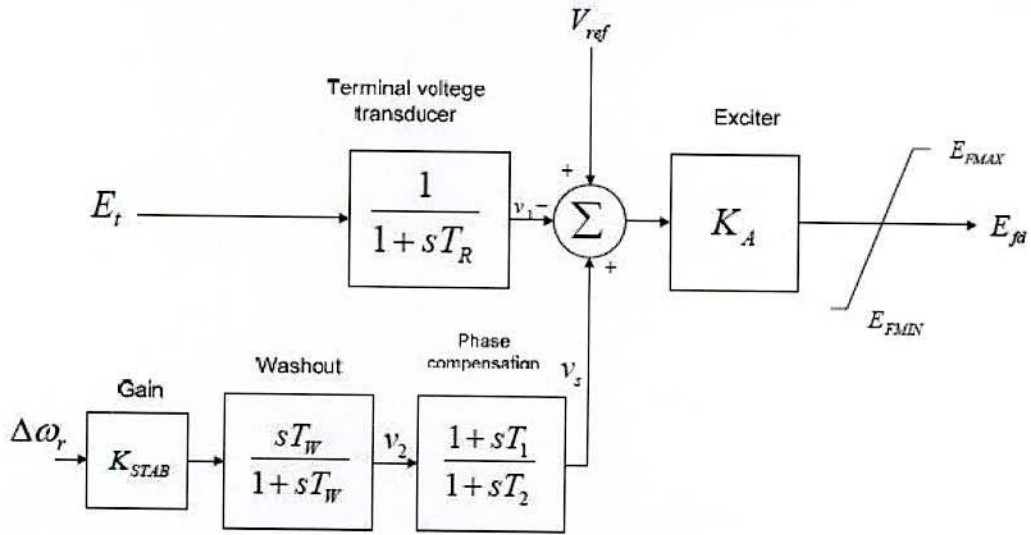


Figure 2.4: Thyristor excitation system with AVR and PSS

2.6 Dynamic Load

Load modeling has a significant impact on power system dynamic analysis results [30]. Accurate load models can result in precise determination of operational limits. On the other hand, inaccurate load models may lead to a power system being operated in modes that result in system collapse or separation [6, 36]. Load models can be broadly classified as either static or dynamic [31]. A static load model does not depend on time [12], and therefore it relates the active and reactive power at a given time to the voltage and/or frequency at the same instant of time. On the other hand, a dynamic load model describes the load behavior as a function of time and therefore provides a much more accurate tool to be used for dynamic simulations [21]. For small signal analysis, it has been reported that the constant impedance load model tends to overestimate system damping by about 25% when compared with a more accurate load representation [36]. The simulations clearly shows that simulations do not reproduce the undamped behavior of the highly stressed power system when motor models are not used and that the use of the motor modeling does reproduce the undamped behavior seen in reality [37]. The induction motor loads which are considered as dynamic loads, account for a large portion of electric loads, especially in large industries and air-conditioning in the commercial and residential areas [36].

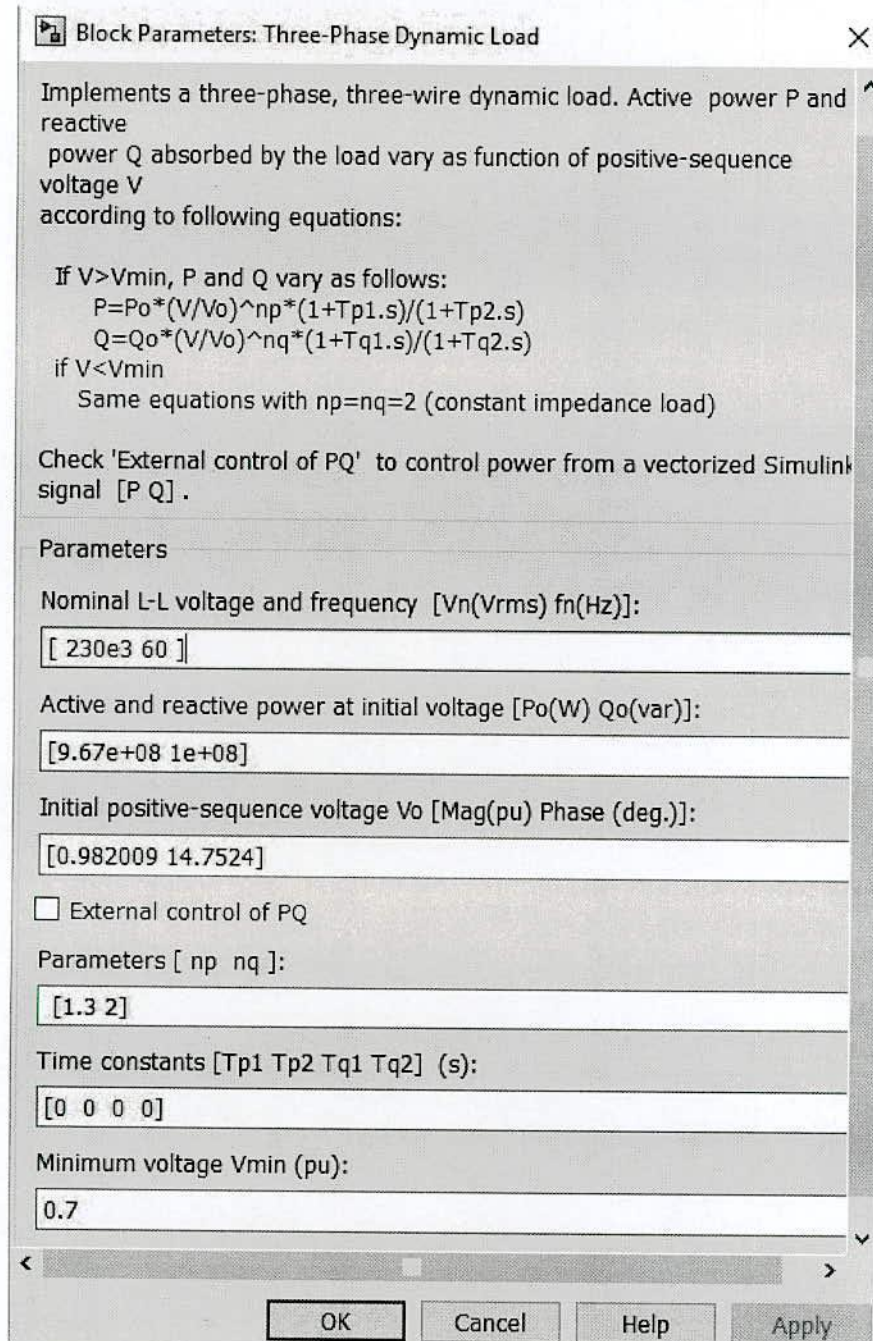


Figure 2.5: Three phase dynamic load block

2.6.1 Exponential Dynamic Load Model

The three phase dynamic load block in simpower implements a three phases three wire whose active power (P) and reactive power (Q) vary as a function of positive sequence voltage. Figure 2.5 shows the three phase dynamic load block. The three loads current are balanced under unbalanced load voltage conditions. The load impedance is kept constant if the terminal voltage V of the load is lower than a specified value V_{min} . The active power (P) and reactive power (Q) of the load vary as [34]:

$$P(s) = P_0 \left(\frac{v}{v_0} \right)^{np} \left(\frac{1 + sT_{p1}}{1 + sT_{p2}} \right) \quad (2.12)$$

$$Q(s) = Q_0 \left(\frac{v}{v_0} \right)^{nq} \left(\frac{1 + sT_{q1}}{1 + sT_{q2}} \right) \quad (2.13)$$

Where V_0 is the initial positive sequence voltage.

P_0 and Q_0 are the initial active and reactive powers at the initial voltage V_0 .

V is the positive sequence voltage.

np and nq are exponents controlling the nature of load.

T_{p1} and T_{p2} are the time constants controlling the active power (P).

T_{q1} and T_{q2} are the time constants controlling the dynamics of the reactive power (Q).

For a constant current load np is 1 and nq is also 1, and constant impedance load np and nq are 2 and 2 respectively.

If $V > V_{min}$, the active and reactive vary according to the equation

$$P(s) = P_0 \left(\frac{v}{v_0} \right)^{np} \left(\frac{1 + sT_{p1}}{1 + sT_{p2}} \right) \quad (2.14)$$

$$Q(s) = Q_0 \left(\frac{v}{v_0} \right)^{nq} \left(\frac{1 + sT_{q1}}{1 + sT_{q2}} \right) \quad (2.15)$$

If $V < V_{min}$, the active and reactive vary same as equation (14) and equation (15) along with $n_p = n_q = 2$ (constant impedance load).

2.7 Load Flow and Machine Initialization

In order to start the simulation in steady state with sinusoidal currents and constant speeds, all the machine states must be initialized properly. This is a difficult task to perform manually, even for a simple system. Figure 2.6 shows Load Flow and Machine Initialization block of the Powergui to perform a load flow and initialize the machines. Double-click the Powergui. In the Tools menu, click the Load Flow and Machine Initialization button. A new window appears. In the upper right window there are a list of the machines appearing in the system. Note that for the Bus Type, choose either PV Generator, PQ Generator, or Swing Generator. For synchronous machines normally specify

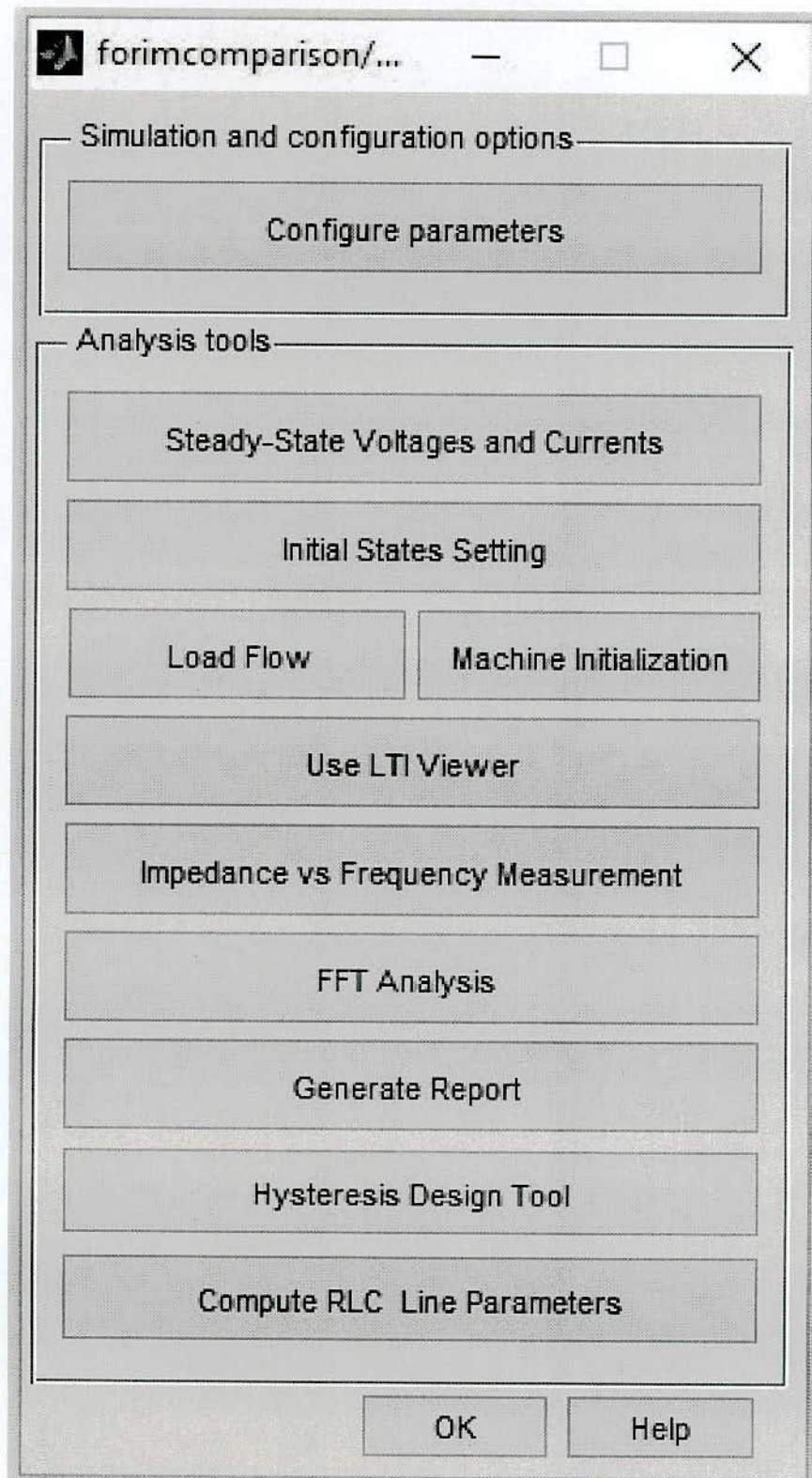


Figure 2.6: Load flow and machine initialization block

the desired terminal voltage and the active power that you want to generate (positive power for generator mode) or absorb (negative power for motor mode). This is possible as long as there is a swing (or slack) bus that generates or absorbs the excess power required to balance the active powers throughout the network. The swing bus can be either a voltage source or any other synchronous machine.

2.8 Conclusion

SimPowerSystems was designed to provide a modern design tool that allows scientists and engineers to rapidly and easily build models that simulate power systems. The libraries contain models of typical power equipment such as transformers, lines, machines, and power electronics. These models are proven ones coming from textbooks, and their validity is based on the experience of the Power Systems Testing and Simulation.

Chapter 3

Conventional Power System Stabilizers

3.1 Introduction

Nonlinear power systems continuously experience generation and load change conditions along with severe disturbances causing change in power system operating conditions [38]. It is essential to keep voltage and frequency of power systems in the desired level with a continuous balance between electricity generation and load demand [1]. Due to the enormous increase in demand for the electricity, the system needs to operate close to the stability limit with quicker and flexible manner in the deregulated competitive environment. These requirements may cause instability as well as low frequency electromechanical oscillations [39]. In this regard, fast excitation control regulates the generated voltage and thus, helps to control steady-state and transient stability of modern synchronous generators [40]. Although AVRs are good to control generated voltage, a high gain excitation system has an adverse effect on the dynamic stability of power system as electromechanical oscillations of low frequencies continue for long time and retard the capabilities of power transfer [2, 9]. In order to improve power system stability, a supplementary stabilizing signal using PSS has been used in AVR to suppress oscillations of low frequency as well as to improve damping of a synchronous generator [10].

Many techniques and approaches have been put to provide the damping torque required for improving the power systems stability such as root locus design method, frequency response techniques, lag-lead compensator which are known as conventional PSS (CPSS). The CPSS parameters are derived from eigenvalue analysis which is iterative and needs huge computations [10, 25]. Furthermore, because of nonlinear behavior of power systems configurations, parameters are changed from time to time [41]. Therefore, they are not able to give optimal solution over wider ranges of operating circumstances. A Fuzzy Logic PSS (FLPSS) has been employed to improve the performance of power systems [9]. The advantage of fuzzy logic is there is no need of mathematical model of the system [26]. However, in FLPSS membership functions (MFs) are set according to trial and error method. On the other hand, during modeling, it cannot be predicted what the MFs should look like simply from looking at data [26]. In this regard, the requirement of an Adaptive Neuro-Fuzzy Inference System (ANFIS) is obvious [13]. An ANFIS based PSS is a new and promising method in which the MFs and rules are adjusted adaptively on the basis of input-output data given as training data to ANFIS [15]. This method is

a combination of fuzzy logic with neural networks [42]. As there are many techniques of PSS design, the comparative analysis among different types of PSS is important to select a suitable design technique for improving the performance of power systems.

3.2 Heffron-Phillips Model of Single Machine Infinite Bus System

Heffron-Phillips model of SMIB system shown in Figure 3.1 is used here [1]. Here, K_S is synchronizing coefficient, K_D is damping torque coefficient, H is inertia constant, $\Delta\omega_r$ is deviation of speed, ω_o is rated speed, s is laplace operator, G_{ex} is representing the transfer function of AVR and exciter and K_1 to K_6 are known as K constants, K_A is exciter gain, T_R , T_3 , and T_A are time constant of voltage transducer, field circuit, and exciter, respectively. An AVR introduces synchronizing torque and damping torque which solely depends on constant K_5 . The numerical values of the constants are given in Appendix.

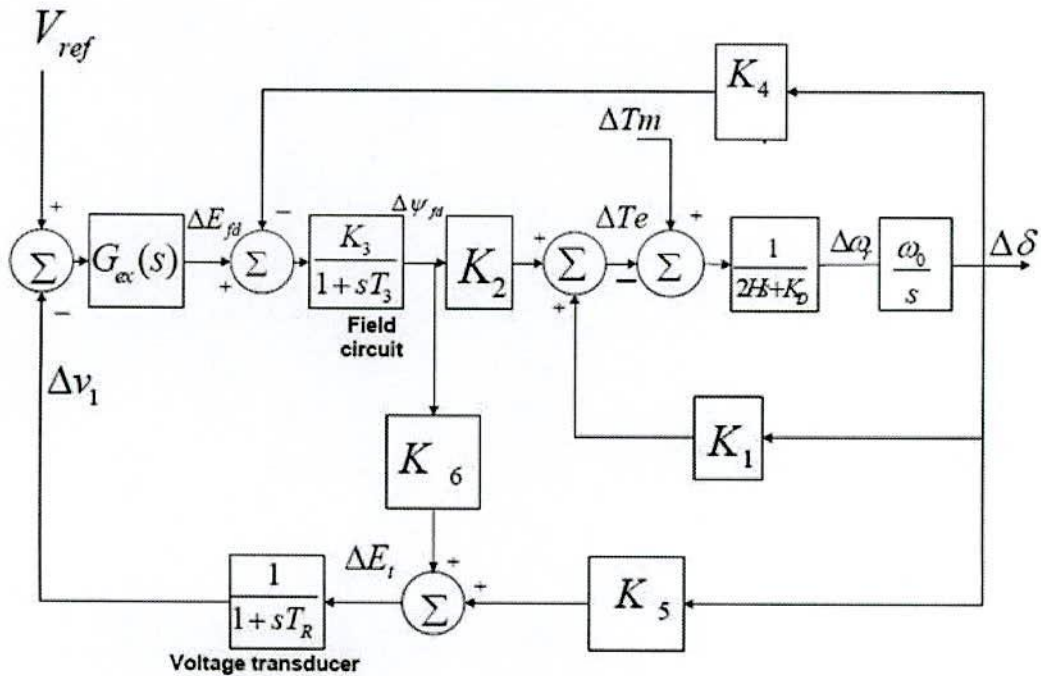


Figure 3.1: Block diagram of SMIB system.

3.3 Proportional Integral Derivative (PID) Controller based AVR

The Simulink structure of single machine infinite bus system with PID controller as AVR is shown in figure 3.2. The input signal to a PSS is speed which is derived from the machine speed passed through a washout filter and several banks of torsional filters. The washout filter is a high-pass filter having a dc gain of 0. The transfer function of washout filter is $10s/(10s+1)$. The torsional filter block filters out the high frequency oscillations due to the torsional interactions of the alternator. One, two or more first order block may be used to achieve desired phase compensation. The transfer function model of this filter is $(1/1 + 0.06s + 0.0017s^2)$. An AVR keeps constant terminal voltage as well as regulates real power flow. An AVR with PID controller improves dynamic response and reduces steady-state error. It improves transient response by padding finite zeros to the plant open loop transfer function (TF) [43]. It increases system type by adding a pole at the origin. The TF of PID controller is

$$G_c(s) = K_P + K_I\left(\frac{1}{s}\right) + K_D s \quad (3.1)$$

A PID controller is added in the forward path of AVR. For tuning of PID parameters firstly, the value of K_P is selected and K_I , K_D is adjusted to some value and then simulation is performed to observe overshoot and settling time. The tuning process is continued until a suitable response is obtained. The values of K_P , K_I and K_D are 1, 0.25 and 0.28, respectively. The block diagram of AVR with PID controller is shown in Figure 3.2.

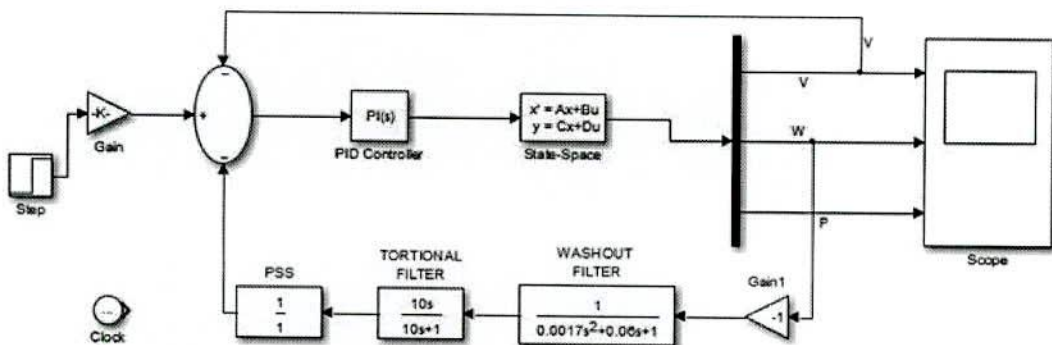


Figure 3.2: Simulink structure of SMIB with PID as AVR.

3.4 Root Locus Design

It involves the design of a Proportional Integral (PI) controller as an AVR and PSS using root locus.

3.4.1 Design of AVR

At the starting point of this method, the AVR loop is replaced by a PI controller and controller parameters are being selected on the basis of time rise (t_r) and maximum overshoot (Mp) which must be less than 0.50 sec and 10%, respectively [44,45]. Then the step response of the regulator loop is drawn from which steady-state error is examined. Figure 3.3 shows the step response for 0.1pu step input and different values of K_i . For $K_p = 35$ and $K_i = 0.6$ the required condition is satisfied. From the above plot, it is clear that there are steady state error and oscillation due to swing mode. Hence, to reduce oscillation a PSS is introduced in the feedback path with angular speed is taken as input. Therefore, a PSS has to be designed by root locus technique.

3.4.2 PSS Design using Root Locus

The root locus of close loop AVR and PSS is drawn and analyzed to find out the complex dominant pole. Figure 3.4 shows the root locus plot of closed loop AVR with PSS. It is found that the dominant complex poles are at $-0.4801 \pm 9.332i$. From the above pole using MATLAB compute departure angle (Φ_p) from the pole and it is $\Phi_p = 43.28$ [44]. According to the value of departure angle the order and parameters of phase lead compensator is chosen. Here, it is needed to add an angle of 137 which cannot be done using a single lead compensator. Therefore, two lead compensators in series each adding an angle of 68.5 is used, having transfer function in the form

$$p(s) = k[k_a \left(\frac{s+z}{s+p} \right)] \quad (3.2)$$

such that $\Phi_p = 180$ [44]. K is chosen from the root locus plot of the final PSS loop such that damping ratio $\tau > 15\%$. The final transfer function of PSS block is $0.4[13.8(s+3.5)/(s+24)]^2$. Finally, the root locus and response of SMIB system using this PSS is redrawn and examined. Figure 3.4. shows the uncompensated system root locus plot having dominant complex pole $-0.4801 \pm 9.332i$ and Figure 3.5 shows the final compensated system root locus plot [44].

3.5 Frequency Response Design

A frequency response design utilizes bode plot to measure gain margin (Gm), phase margin (Pm), DC gain and compensating phase by adding lag controller in the AVR and lead controller in the PSS loop [45].

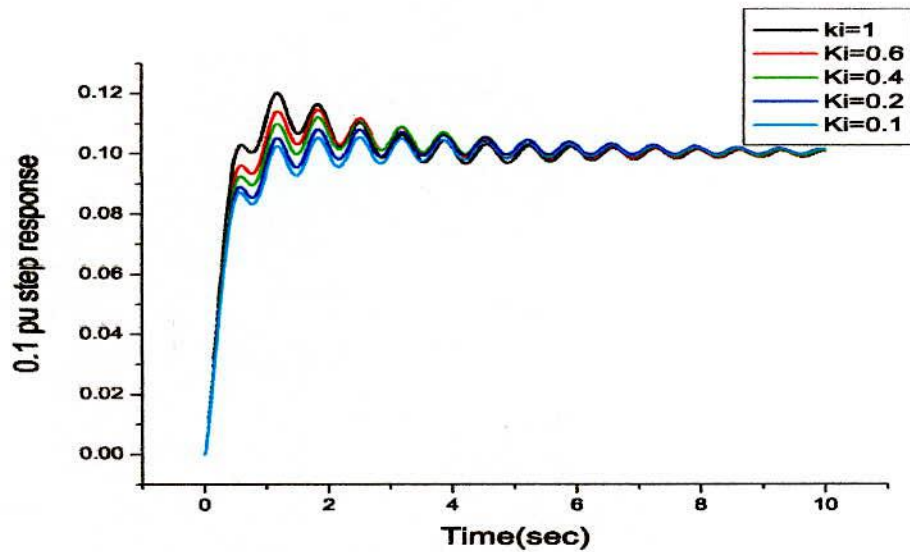


Figure 3.3: Step response for 0.1pu step input and different values of K_i .

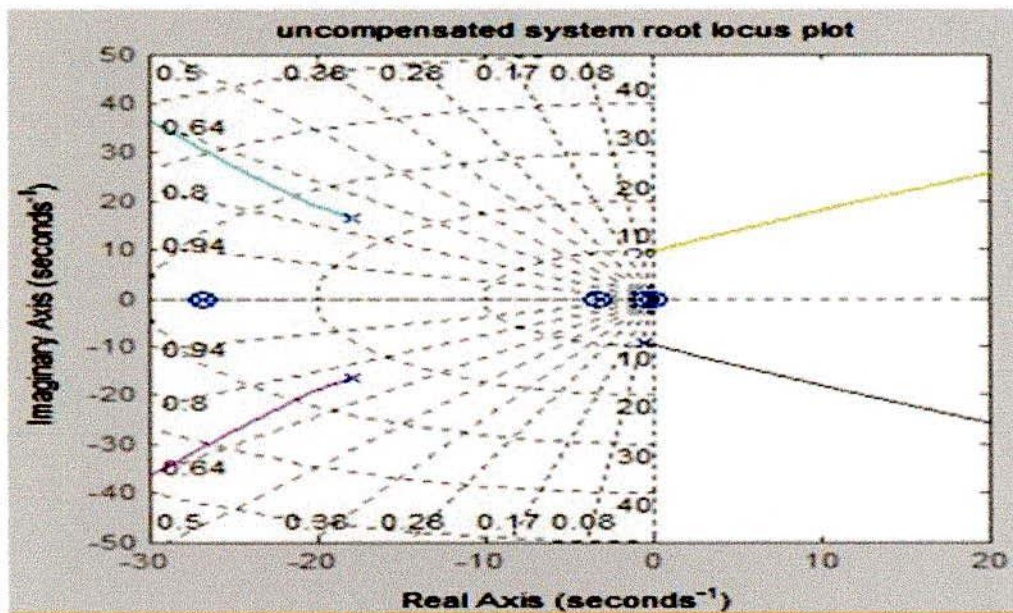


Figure 3.4: Uncompensated system root locus.

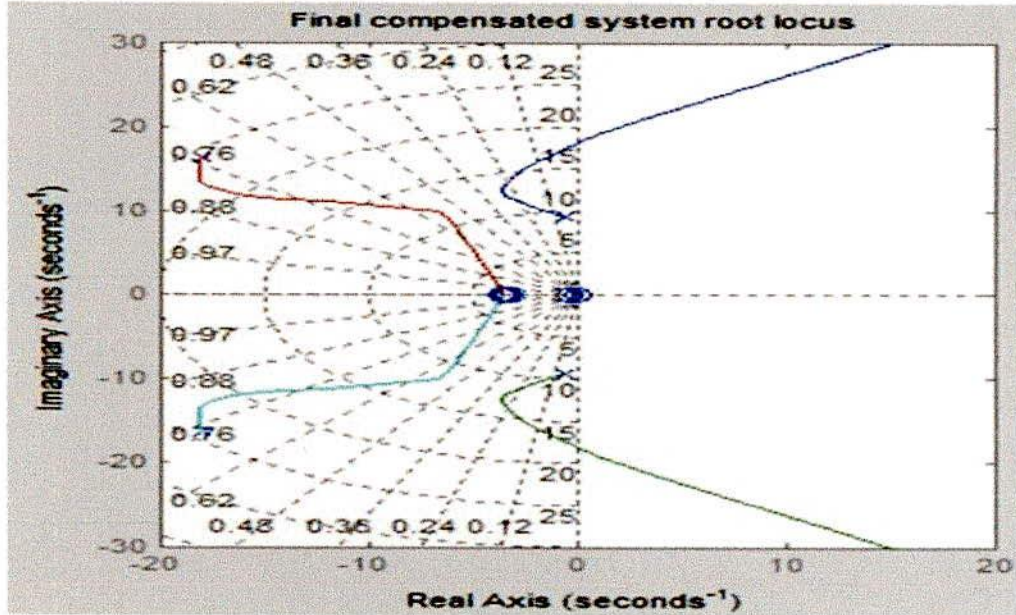


Figure 3.5: Final compensated system root locus plot.

3.5.1 Design of AVR

The frequency response plot of uncompensated system in Figure 3.6 shows the dc gain (-2.59dB) 0.74 and magnitude peak at 9.3 rad/sec. A phase lag AVR has to be designed provided that dc gain must be greater than 200 and phase margin must be greater than 80° [45]. Thus the required gain

$$K_c = 10^{(200+0.74)/20} = 269 \quad (3.3)$$

At this stage, the new gain crossover frequency is determined. To provide the required phase lag to the system at the crossover frequency, a lag-compensator is used as the AVR, having transfer function [44]

$$K(s) = K_l \left(\frac{s+z}{s+p} \right) \quad (3.4)$$

$$\text{compensator gain, } K_l = K_c/\beta \quad (3.5)$$

$$p = z/\beta \quad (3.6)$$

Now, the lag required at 5rad/sec is -18dB.

$$\text{Hence, } 20 \log \frac{1}{\beta} = -18, \text{ therefore } \beta = 8 \quad (3.7)$$

The resultant phase lag AVR is $35(s+0.1)/(s+0.0125)$. Now step response is determined by adding the AVR loop. Figure 3.7 shows the step response of lag compensator as AVR for 0.1pu step input where $t_r = 0.4810$ sec and $M_p = 6.7941\%$ are obtained.

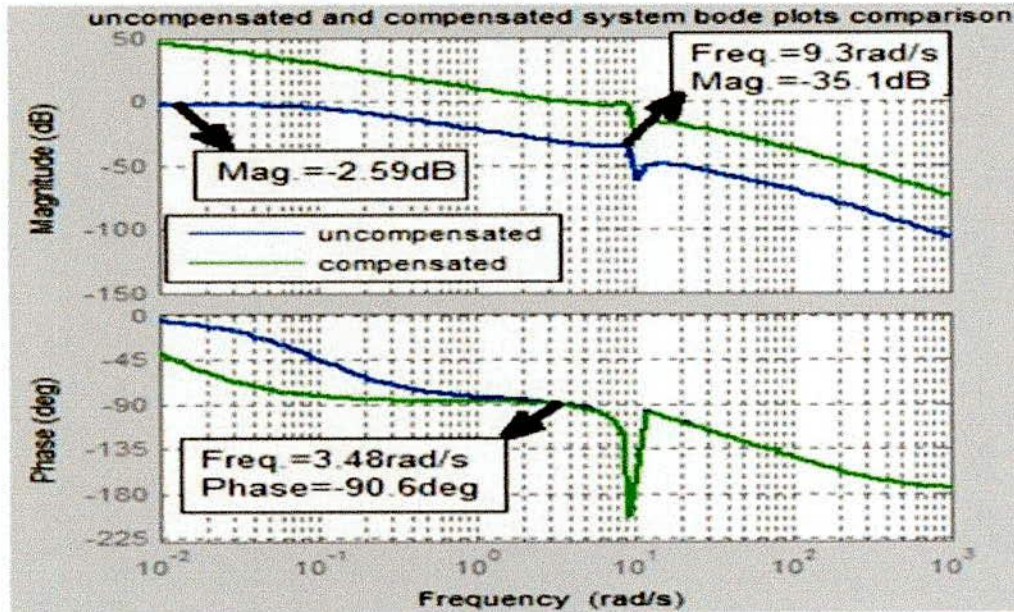


Figure 3.6: Frequency response plot with and without VR loop.

3.5.2 Design of PSS

The state-space model is generated from V_{ref} to $\omega(speed)$ with the regulation loop closed and the model is decomposed to isolate the $Q(s)$ path from the speed to electrical torque (effect of speed on electric torque due to machine dynamics) to obtain new matrix A_w from the original matrix A , and this is shown in Figure 3.8. The resulting system matrix A_w has the form

$$A_w = \begin{bmatrix} 0 & 377 & 0 \\ -K & D & a_{23} \\ a_{31} & a_{32} & a_{33} \end{bmatrix} \quad (3.8)$$

where $K=0.2462$, $D=0.15$, a_{32} is a row vector, and a_{31} and a_{33} are column vectors, and is a square matrix. These values are given in appendix. In the next step, resulting state space model is converted to transfer function and $Q(s)$ is connected with torsional filter and washout filter to get $F(s)$. The frequency response plot of $F(s)$ is shown in Figure 3.9, which shows phase at 2 rad/sec is -37 and phase at 20 rad/sec is -105. Therefore,

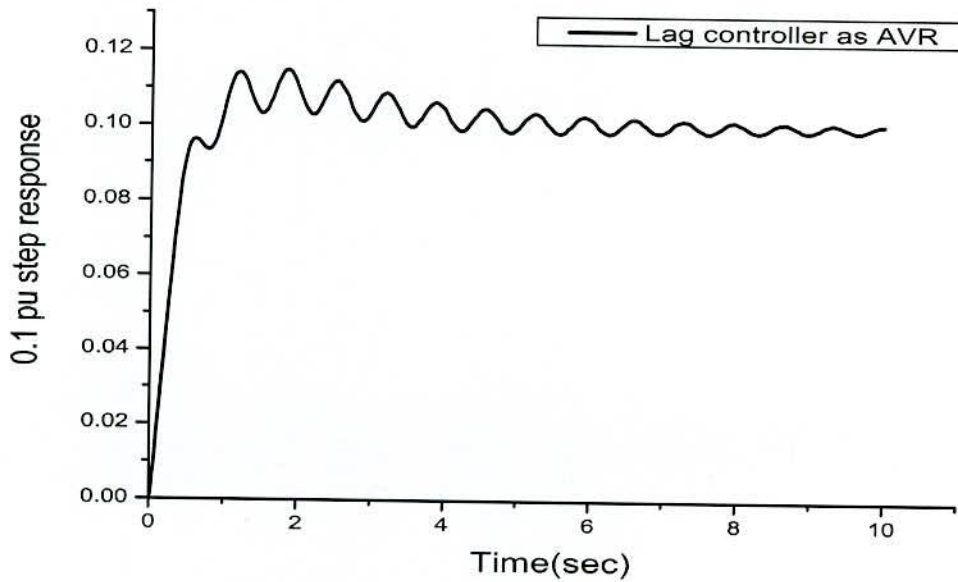


Figure 3.7: Step response of lag compensator as voltage regulator for 0.1 pu step input.

a phase lead controller has to be designed which increases this phase at 2 to 20 rad/sec from the above values to approximately 0 to -15, such that the feedback loop adds pure damping to the dominant poles. It needs an additional phase of 35 at 2 rad/sec, 60 at 12 rad/sec, and 100 at 20 rad/sec [44]. Here, maximum phase addition Φ_m is 100 at 20 rad/sec which is too large for a single lead compensator. Therefore, two compensator are used in series, having transfer function [44]

$$V(s) = K \left[K_\alpha \frac{s+z}{s+p} \right] \left[K_\alpha \frac{s+z}{s+p} \right] \quad (3.9)$$

where,

$$\sin \phi_m = \frac{1-\alpha}{1+\alpha}$$

$$T = \frac{1}{\sqrt{\alpha\omega}}$$

$$z = \frac{1}{T}$$

$$p = \frac{1}{\alpha T}$$

$$K_\alpha = \frac{1}{\alpha}$$

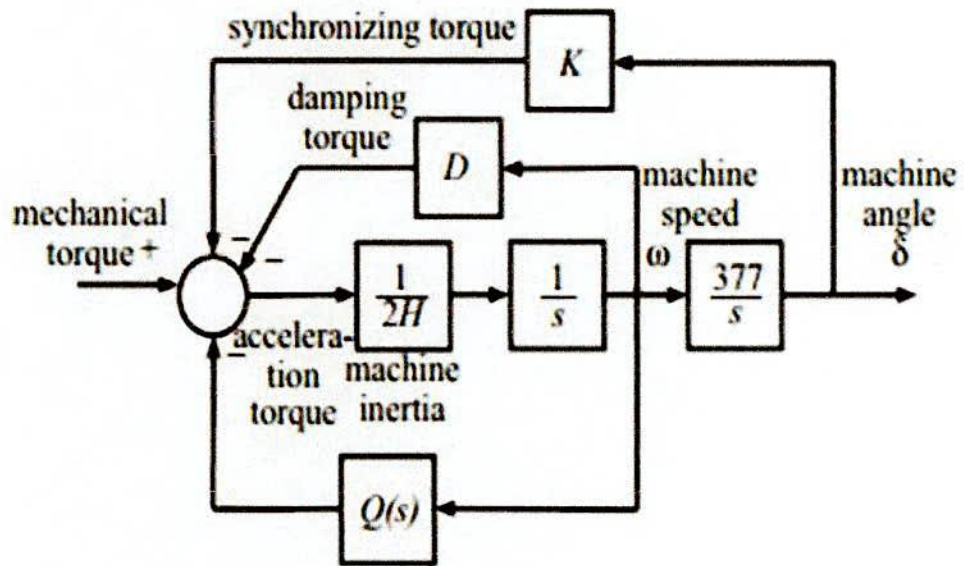


Figure 3.8: Separation of speed control loop.

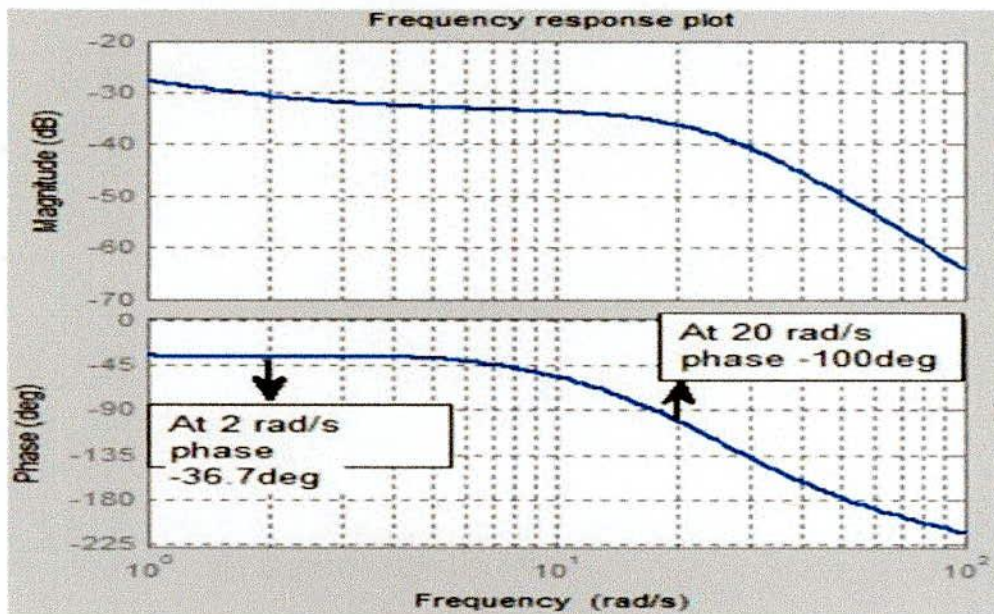


Figure 3.9: Frequency response of damping loop.

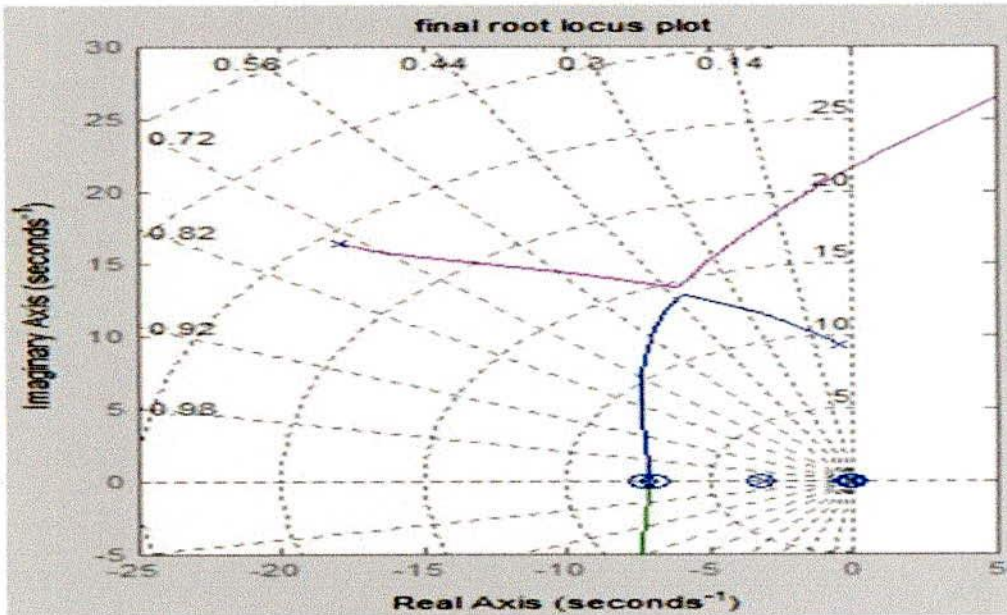


Figure 3.10: Root locus of PSS loop with compensator.

3.6 PSS Design using Artificial Intelligence

3.6.1 FLPSS Design

It is generally a rule base system that executes a control decision on the basis of fuzzy rules [46]. A fuzzy inference system of FLC maps the given input to fuzzy variables, fuzzy variables to rule to produce consequent fuzzy region for each variables, and finally, defuzzified outputs. The FLPSS input signals are speed deviation of rotor and acceleration and voltage stabilization signal to exciter is the output. Seven triangular linguistic fuzzy subset for each of the input-output variables are used [46]. The abbreviations of seven linguistic variables are respectively NB (Negative Big), NM (Negative medium), NS (Negative Small), ZE (Zero), PS (Positive Small), PM (positive Medium) and PB (Positive Big). The detail design procedure of FLPSS is given in the chapter IV. Two inputs, speed deviation and acceleration generate 49 rules that define the relation between input and output of fuzzy controller. Thus, the stabilizing signals have been computed [47]. The rule base of fuzzy logic controller is shown in Table I. The matlab simulink model of SMIB with fuzzy logic controller is shown in figure 3.11. The design procedures of FLPSS are as follows:

- Select input and output variables.
- Select MFs.
- Set up fuzzy rule.

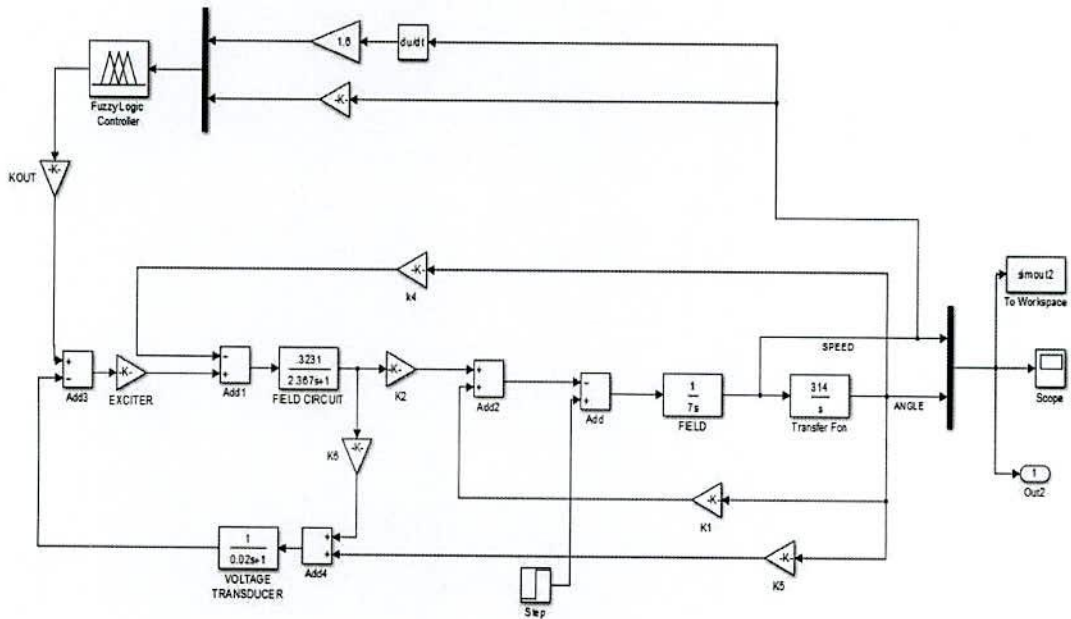


Figure 3.11: Matlab/Simulink model of SMIB with fuzzy logic controller.

- Finally, choose defuzzification criteria.

3.6.2 ANFIS based PSS Design

An ANFIS-PSS is an artificial neural network based approach which shows great potential of damping low frequency electromechanical oscillations. Its design process can be divided into two steps. Firstly, input-output data pair of the system is generated using FLPSS which is called training data. This training data determines the exact relation between input and output of ANFIS-PSS. Then, a fuzzy inference system (FIS) is created. FISs MF parameters tend to be adjusted with the use of either only a backpropagation algorithm, or in a permutation with a least squares method [47]. Gaussian MFs have been used here. After selecting number of MFs, MFs types, number of training epoch, and expectable training error, the network is trained. Finally, if the FIS model is valid, it is saved. Two inputs, rotor speed change ($\Delta\omega_r$) and rotor acceleration ($\Delta\dot{\omega}_r$), and a Takagi-Sugeno type FIS model are used here. The inputs are Gaussian membership type. Seven MFs are required to cover the full range of respective inputs. In this way, 49 rules appear for the output function which demonstrate a linear relation to the inputs. The detail design procedure of ANFIS-PSS is given in the chapter IV. The design procedure of ANFIS-PSS is as follows.

- Firstly, generate training data by using FLPSS.
- Then generate FIS system.

- Select number of MFs, types, epoch number and maximum training error.
- Then start training and observe training error.
- Continue training until training error is within expected level.
- Then check model validation.
- Finally, save FIS structure.

3.7 Simulation Results

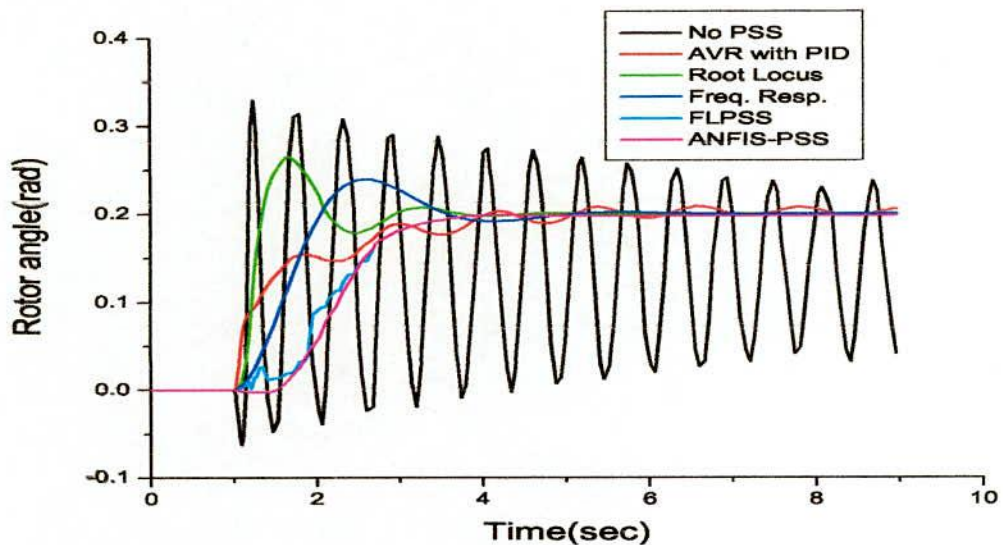


Figure 3.12: Response of rotor angle for a 5% change in mechanical input.

To analyze the performance of the designed PSS, a time-domain simulation is carried out. The mechanical input to the generator is increased (5%) at 1 sec. The response of rotor angle and speed deviation of the synchronous generator for different types of controller is shown in Figure 3.12 and Figure 3.13, respectively. An AVR is suitable for regulation of generated voltage but it introduces low frequency oscillations and persists for a long period of time. Therefore, a PSS is needed. The performance of root locus and frequency response PSS is quite good. However, they suffer from overshoot and undershoot and take more time to settle down. It is to be mentioned that CPSS parameters are tuned and works well for a particular operating conditions. A FLPSS shows better performance compared to CPSS, however, MF selection is a tough task for it. From the comparison, it can be observed that an ANFIS-PSS shows better performance

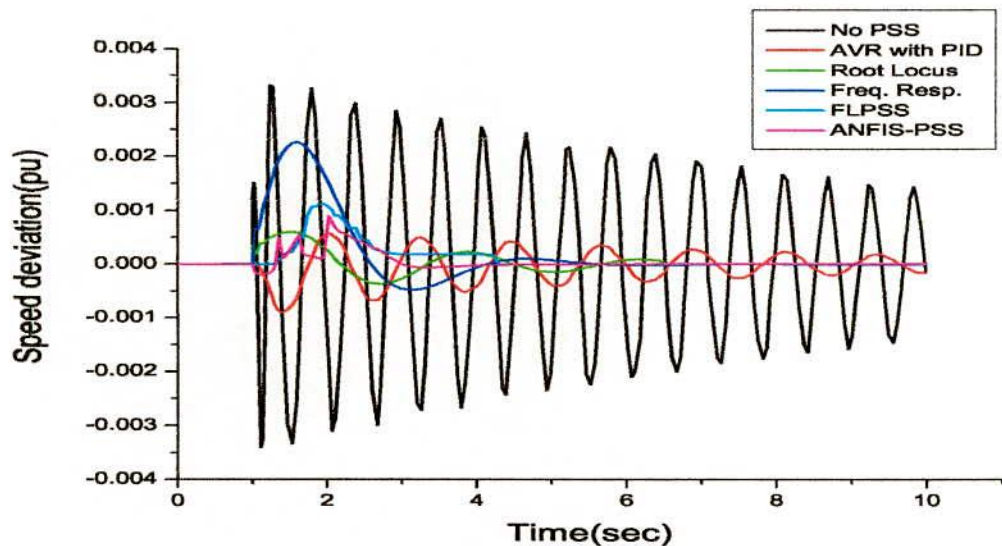


Figure 3.13: Response of rotor speed deviation for a 5% change in mechanical input.

in all respect. The main advantage of the ANFIS controller is its robustness and design simplicity. The ANFIS-PSS adjusts its parameters adaptively on the basis of given input-output data to the controller as training data.

3.8 Conclusion

The performance of different types of PSS design method is analyzed. It is found that a generator without any PSS has large angle and speed deviation. It is found that conventional design method of PSS cannot guarantee satisfactory performance under varying operating conditions. Although fuzzy logic controller can enhance the systems performance, there are no definite criteria for selection of its MFs. However, the designed adaptive PSS can overcome the aforementioned difficulties. Simulation results show that the ANFIS-PSS ensures the best performance in terms of setting time and overshoot when operating condition changes. Therefore, it can be effectively used for modern power system applications.

Chapter 4

Design of a PSS Using ANFIS for a Multi-Machine System Having Dynamic Loads

4.1 Introduction

The conventional PSSs (referred to as CPSS) parameters are derived from a linearized model of the power system [25]. Furthermore, CPSSs work well with those specific operating points of the system for which they are modeled. Because of nonlinear behavior of power systems, configurations and parameters are changed from time to time, so they are not able to give acceptable results over wider ranges of operating circumstances. In recent times, with the revolutionary advancement in digital computers, it is easy to implement novel controllers utilizing intelligent control approaches. FLPSSs have been employed to improve the performance of conventional PSSs. It is generally a rule based system. Complex and nonlinear problems are made easier to solve by FLC without knowing the accurate mathematical model of the systems [26]. In view of the fact that the FLPSS shows good performance, there is no orderly design procedure for the fine-tuning of the parameters of it. Moreover during modeling, it cannot be guessed which types of membership functions (MFs) should be employed from analyzing the data [26]. Therefore, the design of FLPSS becomes a tough job. On the other hand, ANFIS based technique is a promising method, which adjusts membership functions and rules adaptively to improve the systems performance [15]. This work introduces a PSS for a multi-machine interconnected power system comprising a dynamic load grounded on adaptive-neuro fuzzy technique. There is a rich literature on the PSS design considering static load [9, 25, 26, 41]. As loads play an important role in power system stability study [28, 29], the incorporation of load dynamics during a PSS design is essential. Therefore, the aim of the proposed research is to investigate the performance of ANFIS-PSS in the presence of a dynamic load in the system.

4.2 Fuzzy Logic Controller

The fuzzy control system is rule based system in which a set of fuzzy rules represent a control decision mechanism to adjust the effects of certain system stimuli. The fuzzy

logic controller comprises four principle components: fuzzification interface, knowledge base, decision making logic, and defuzzification interface. The basic structure of FLC is shown in figure 4.1 [46]. The system input received by the FLC is turned into fuzzy form. On the basis of fuzzy rules, input, and MFs, the controller obtains the output in fuzzy form and finally, turns the output in nonfuzzy form [46,48]. In fuzzification, the values of input variables are measured i.e. it converts the input data into suitable linguistic values, which may be viewed as label fuzzy sets. The knowledge base consists of a database and linguistic control rule base. The database provides the necessary definitions, which are used to define the linguistic control rules and fuzzy data manipulation in an FLC. The rule base characterizes the control policy of domain experts by means of set of linguistic control rules. The decision making logic has the capability of stimulating human decision making based on fuzzy concepts. The defuzzification performs scale mapping, which converts the range of values of output variables into corresponding universe of discourse. Maximum method, height method, centroid method are the three efficient techniques for defuzzification.

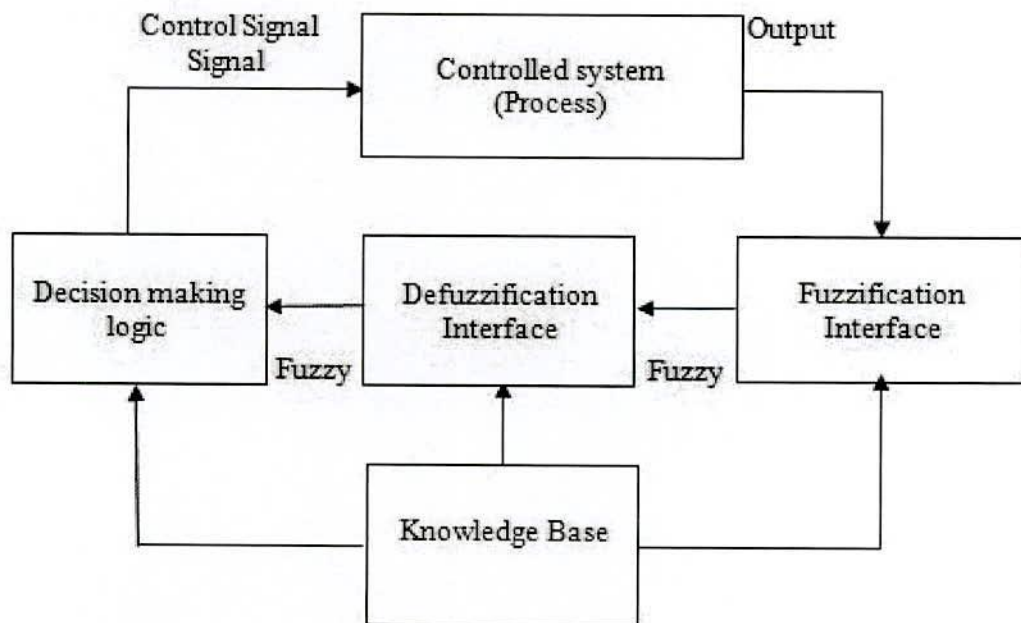


Figure 4.1: FLC structure

4.3 Fuzzy Sets

Membership function has an important role in fuzzy set. Fuzzy set is a set without a crisp boundary. The transition from belong to a set to not belong to a set is gradual, and this smooth transition is characterized by membership functions. The fuzzy set theory is based on fuzzy logic, where a particular object has a degree of membership in a given set that may be anywhere in the range of 0 to 1. On the other hand, classical set theory is based on Boolean logic, where a particular object or variable is either a member of a given set (logic 1), or it is not (logic 0). A and B are two fuzzy sets with membership functions $v_a(x)$ and $v_b(x)$, respectively then [9]

The union of two fuzzy sets;

- $v_c(x) = \max[v_a(x), v_b(x)]x \in X$

The intersection of two fuzzy sets;

- $v_c(x) = \min[v_a(x), v_b(x)]x \in X$

The compliment of a fuzzy set;

- $v_a(x) = 1 - v_a(x)x \in X$

4.4 Membership Functions

A membership function is a curve that defines how the values of a fuzzy variable in a certain region are mapped to a membership value (or degree of membership) between 0 and 1. The MF maps each element of X to a membership degree between 0 and 1. Obviously, the definition of a fuzzy set is a simple extension of the definition of a classical (crisp) set in which the characteristic function is permitted to have any value between 0 and 1. If the value of the membership function is restricted to either 0 or 1, then A is reduced to a classical set. For clarity, we shall also refer to classical sets as ordinary sets, crisp sets, non-fuzzy sets, or just sets. Usually, X is referred to as the universe of discourse, or simply the universe, and it may consist of discrete (ordered or non-ordered) objects or it can be a continuous space. In practice, when the universe of discourse X is a continuous space, it is usually partitioned into several fuzzy sets whose MFs cover X in a more or less uniform manner. These fuzzy sets, which usually carry names that conform to adjectives appearing in our daily linguistic usage, such as large, medium, or small, are called linguistic values or linguistic labels. Thus, the universe of discourse X is often called the linguistic variable. The fuzzy membership not only provides for a meaningful and powerful representation of measurement of uncertainties, but also provides the meaningful representation of vague concepts expressed in natural language [48]. If X is a collection of objects denoted generically by x, then a fuzzy set in X is defined as a set of ordered pairs.

$$A = \{(x; \mu_A(x))/x \in X\}$$

where $\mu_A(x)$ is called the membership function for the set A .

There exist different shapes of membership functions. The shapes could be triangular, trapezoidal, curved or their variations. There are various types of membership functions like

- Triangular Membership Function
- Gaussian Membership Function
- Trapezoidal Membership Function
- Sigmoidal Membership Function
- Generalized bell Membership Function

4.5 Implication Methods

There are number of implication methods to fuzzy logic, but only two widely used methods are discussed here. Those are Mamdani type fuzzy model and Sugeno type fuzzy model. Mamdani fuzzy rule for a fuzzy controller involving three input variables and two output variables can be described as follows: IF x_1 is A AND x_2 is B AND x_3 is C THEN z_1 is D, z_2 is E. where x_1 , x_2 , and x_3 are input variables (e.g., error, its first derivative and its second derivative), and z_1 and z_2 are output variables [48]. These variables are discrete because virtually all fuzzy controllers and models are implemented using digital computers. A, B, C, D and E are fuzzy sets. IF x_1 is A AND x_2 is B AND x_3 is C is called the rule antecedent, whereas the remaining part is named the rule consequent. The structure of Mamdani fuzzy rules for fuzzy modeling is the same. The variables involved, however, are different. The Sugeno fuzzy model or TSK fuzzy model was proposed by Takagi, Sugeno, and Kang and was introduced in 1985. A typical fuzzy rule in a Sugeno fuzzy model has the form

- IF x is A and y is B then, $z = f(x, y)$;

where A and B are fuzzy sets in the antecedent, while $z = f(x, y)$ is a crisp function in the consequent. Usually $z = f(x, y)$ is a polynomial in the input variables x and y , but it can be any function as long as it can appropriately describe the output of the model within the fuzzy region specified by the antecedent of the rule. When $z = f(x, y)$ is a first-order polynomial, the resulting fuzzy inference system is called a first-order Sugeno fuzzy model. When f is a constant, we then have a zero-order Sugeno fuzzy model [48].

4.6 Controller Design Procedure

The design steps of FLC are as follows

- Define input and output variables

- Choice of linguistic variables
- Selection of fuzzy rule
- Defuzzification action

4.7 Fuzzy PSS Design in Mamdani Form

As a first line of FLPSS design input signals to the controller are selected which characterize the dynamic performance of the system. In this thesis, a Mamdani form of FLC is used which has two inputs and one output component. Inputs to the FLC are the generator rotor angular speed deviation ($\Delta\omega_r$) and change of speed deviation ($\Delta\dot{\omega}_r$) and the output is voltage (V_{PSS}). Seven linguistic fuzzy subset for each of the input-output variables are used [46, 47]. The linguistic variables are given in table 4.1. Two inputs ($\Delta\omega_r$), and ($\Delta\dot{\omega}_r$), generate 49 rules that define the relation between input and output of FLC. Thus, the stabilizing signals have been computed [47]. The rule table of FLC is shown in table 4.2 [47]. Given that the exciter needed a non-fuzzy signal, the centroid defuzzification approach is used to obtain output. The MFs for inputs and output are shown in figure 4.2 to figure 4.4.

Table 4.1: Linguistic Variables of FLC

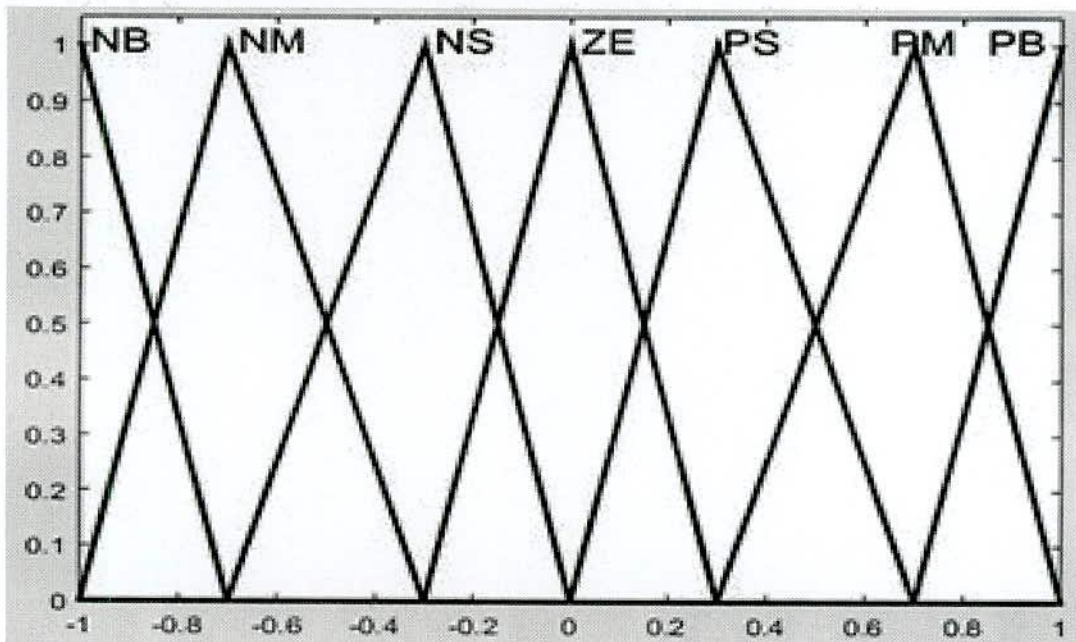
NB	Negative Big
NM	Negative Medium
NS	Negative Small
ZE	Zero
PS	Positive Small
PM	Positive Medium
PB	Positive Big

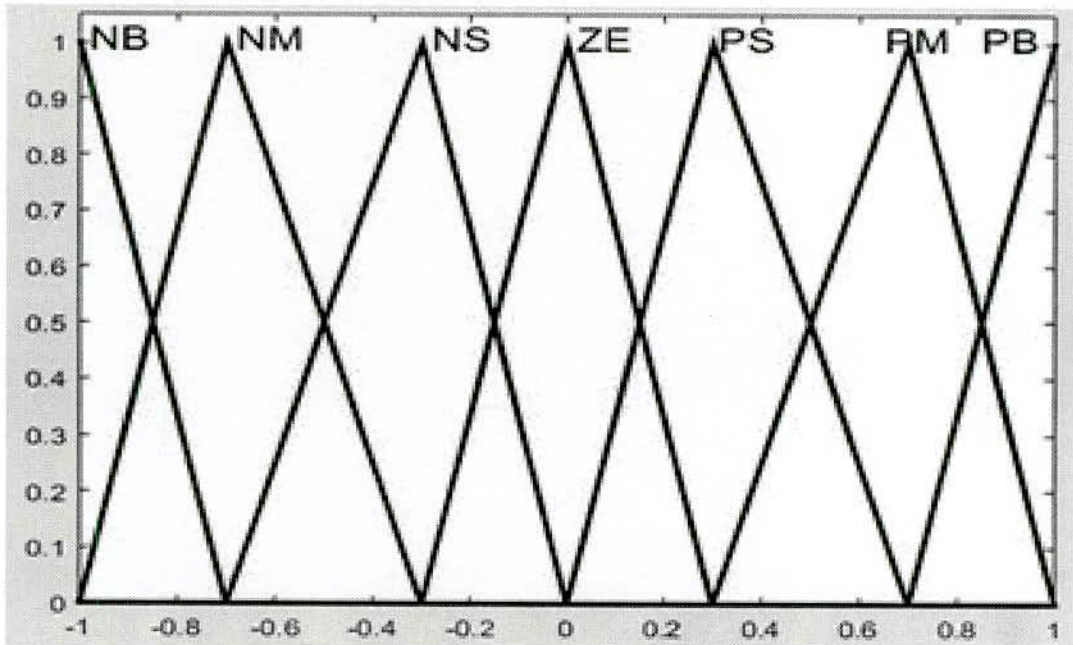
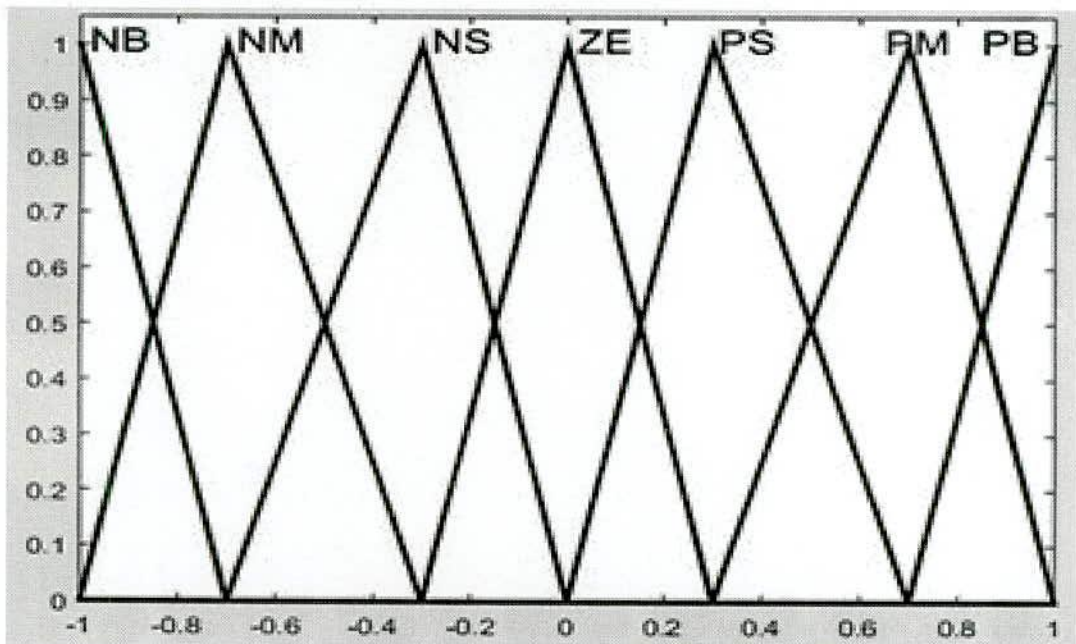
4.8 Artificial Neural Networks

An artificial neural network is a mathematical model or computational model based on human neural networks. It consists of a number of simple nodes connected together to form either a single layer or multiple layers. The connections between nodes also termed neurons are called weights that should be adjusted to reach the desired target [7]. Figure 4.5 shows the ANFIS structure consists of 5 layers [7]. Figure 4.6 shows the triangular fuzzy set. In this structure, the circle indicates a fixed node whereas a square indicates an adaptive nodes, which implies that the parameters are changed during training. Learning

Table 4.2: Rule Table of FLC

$\Delta\omega_r$	$\Delta\dot{\omega}_r$						
	NB	NM	NS	ZE	PS	PM	PB
NB	NB	NB	NB	NB	NM	NM	PS
NM	NB	NM	NM	NM	NS	NS	ZE
NS	NM	NM	NS	NS	ZE	ZE	PS
ZE	NM	NS	NS	ZE	PS	PS	PM
PS	NS	ZE	ZE	PS	PS	PM	PM
PM	ZE	PS	PS	PM	PM	PM	PB
PB	PS	PM	PM	PB	PB	PB	PB

Figure 4.2: Input MF ($\Delta\omega_r$)

Figure 4.3: Input MF ($\Delta\omega_r$)Figure 4.4: Output MF (ΔV_{PSS})

is achieved by combining the back propagation algorithm and the least squares method. Explanation of each Layer are given bellow.

- Layer 1: Fuzzification Layer

This layer is the fuzzification layer which calculates the membership value for Premise parameters A1 to A7 and A1 to B7. The premise parameters can be trained using the hybrid-learning algorithm. All the nodes in this layer are adaptive nodes. $\mu_{A_i}(x)$ and $\mu_{B_i}(y)$ are the triangular membership values for different fuzzy labels A1 to A7 and B1 to B7 which corresponds to the respective input signals $\Delta\omega_r$ and $\Delta\dot{\omega}_r$ [7]. This membership function is given by equation (4.1)

$$\mu_{aj}(x) = \begin{cases} 0 & \text{if } x \leq a - b/2 \\ 1 - \frac{2|x_i - a|}{b} & \text{if } a - \frac{b}{2} < x_i < a + \frac{b}{2} \\ 0, & \text{if } x_i \geq a + \frac{b}{2}, i = 1, \dots, 7 \end{cases} \quad (4.1)$$

where a is the center of the triangular fuzzy set and b is the width of the triangular fuzzy set. a and b are called the premise parameters. Each node in layer 1 is a square node with the node function of equation (4.2)

$$\phi_i^1 = \{\mu_{A_i}(X)\} \text{ and } \phi_i^1 = \mu_{B_i}(X) \text{ for } i = 1, \dots, 7 \quad (4.2)$$

where x and y are the input signals ($\Delta\omega_r$ and $\Delta\dot{\omega}_r$) of the node i .

- Layer 2: Firing Strength layer

This layer represents the firing strength of the rule. The nodes of this layer are called rule nodes. Every node in layer 2 is a fixed node and calculates the firing strength of each rule using AND node function of the combination of the input signals [7]. The output of i th node of layer 2 is given by equation (4.3) as

$$\phi_i^2 = \omega_i = \text{minimum}(\mu_{A_i}(X), \mu_{B_i}(y)); i = 1 \dots 49 \quad (4.3)$$

- Layer 3: Normalization layer

The i th node of layer 3 calculates the normalized firing strength of each rule that is the ratio of the i th rules firing strength to the sum of all rules firing strengths [7]. Nodes in this layer are also fixed nodes. The output of it node of layer 3 is given by equation (4.4) as

$$\phi_i^3 = \bar{\omega}_i = \frac{\omega_i}{\sum_{j=1}^N \omega_j}; i = 1, \dots, 49 \quad (4.4)$$

where N is the no. of rules

- Layer 4: Defuzzification Layer

The nodes in layer 4 are adaptive nodes. The output of each node is simply the product of the normalized firing strength and individual rule output of corresponding rule (r_i) which is also known as consequence parameters [7]. The output of i th node of layer 4 is given by equation (4.5) as

$$o_i^4 = \bar{\omega}_i r_i = \frac{\omega_i}{\sum_{j=1}^N \omega_j} r_i; i = 1, \dots, 49 \quad (4.5)$$

- Layer 5: Summing Layer

This layer has only one that performs the function of a simple summer. This neuron calculates the sum of outputs of all defuzzification neurons and produces the overall ANFIS output [48]. The output of layer 5 is given by equation (4.6) as:

$$o_i^5 = u = \sum_{i=1}^N \bar{\omega}_i r_i = \frac{\sum_{i=1}^N r_i \cdot \omega_i}{\sum_{j=1}^N \omega_j} r_i; i = 1, \dots, 49 \quad (4.6)$$

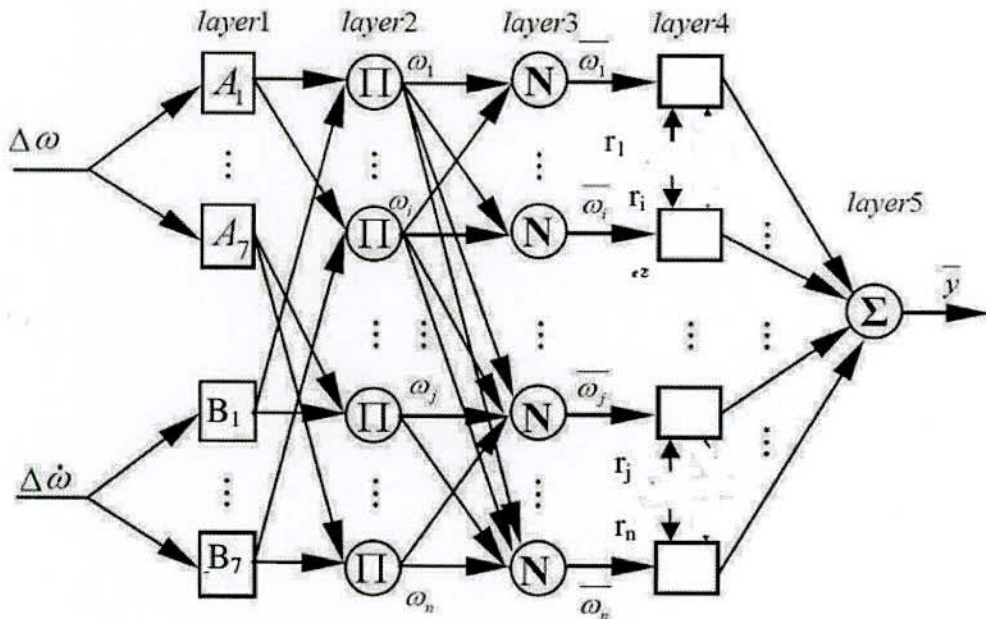


Figure 4.5: The architecture of the ANFIS.

4.9 Training Procedure for ANFIS Network

The training procedure is achieved based on the hybrid learning technique, where the tuning of the ANFIS controller is achieved with the back propagation algorithm using

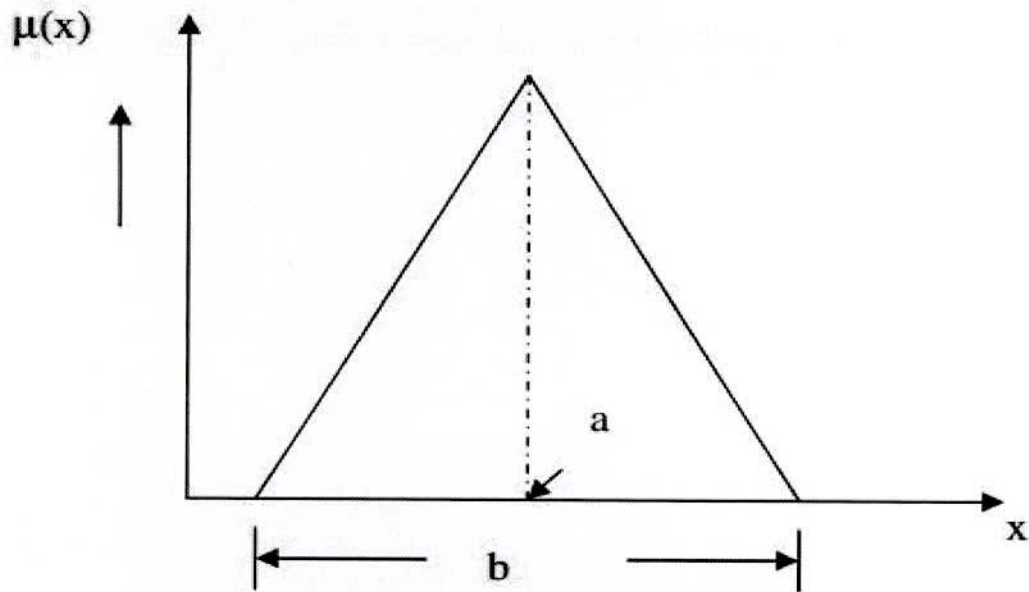


Figure 4.6: Triangular fuzzy MF

input output training data set. The parameters are trained using back propagation and least square estimation method (LSE). The learning algorithm is composed of a forward pass, using the available values of premise parameters, functional signals go till layer 4 and consequent parameter vector is identified by means of LSE. In the backward pass, the error rates propagate backward and premise parameters are updated by the gradient decent. The training data must cover a wide range of operating conditions. The Fuzzy Logic PSS structure is used to obtain the training data. For getting the training data, we input the various $(\Delta\omega_r)$ and $(\Delta\dot{\omega}_r)$ values into the FPSS and get the corresponding output V_{FPSS} . Using these training data, the premise parameters and the consequence parameters of the ANFIS structure are trained. The trained ANFIS structure is ready to be implemented in the power system.

4.10 Hybrid Learning Algorithm

The robust fuzzy neural network proposed is trained by hybrid learning algorithm. The hybrid-based algorithm is based on error back propagation and least squares estimate techniques. The ANFIS based PSS has the property of learning i.e. fuzzy rules and membership functions of the controller can be tuned using a learning algorithm. The output of the network can be evaluated as in equation (4.7).

$$= u = \sum_{i=1}^N \bar{\omega}_i r_i = \frac{\sum_{i=1}^N r_i \cdot \omega_i}{\sum_{j=1}^N \omega_j} r_i; i = 1, \dots, 49 \quad (4.7)$$

4.11 Adaptive-Neuro Fuzzy Controller

An ANFIS editor GUI is available in Fuzzy Logic Toolbox in MATLAB. This toolbar receives input/output data set as input. Thus, it creates a fuzzy inference system (FIS). FISs MF parameters tend to be adjusted with the use of either only a backpropagation algorithm, or in a permutation with a least squares method [44]. The process agrees to the fuzzy systems towards learning from the data they model. At this point of the system, the input-output data pair is generated using the FLPSS structure. Afterwards, a fuzzy inference system is created by using the ANFIS model in MATLAB. Inputs are used, namely $\Delta\omega_r$ and $\Delta\omega_r$, and output is ΔV_{PSS} [47]. In this thesis, a Takagi-Sugeno (T-S) type FIS model is used. The inputs are Gaussian membership type. Seven MFs are required to cover the full range of respective inputs. In this way, 49 rules appear for the output function which demonstrates a linear relation to the inputs. The ANFIS-PSS design follows the steps below.

- Generate input-output data of the system using FLPSS.
- Then create a suitable ANFIS structure for a given challenge.
- Select number of training epoch.
- Using the test patterns train ANFIS until it performs in the expected level.
- Then check the model validation.

Figure 4.7 shows the flowchart of ANFIS-PSS design procedure. Figures 4.8 and 4.9 show the training error and ANFIS structure, respectively.

4.12 Problem Description

The two area multi-machine power system used in this simulation is shown in Figure 4.10 [1]. The test system is modified by connecting a dynamic load at bus 7. Two symmetrical areas are connected through two 230 kV lines of 220 km long transmission lines. Each area has two similar round rotor generators rated at 20kV/900MVA. The inertia constants of generators in area 1 (A-1) and area 2 (A-2) are 6.5s and 6.17s, respectively. A dynamic load rated at 967 MW and 100MVAR is connected in A-1. Similarly, another static load rated at 1767MW, 100MVAR and -187MVAR is connected in A-2. Load voltage is improved by inserting a capacitor of 200MVAR and 350MVAR in A-1 and A-2, respectively. In the next section, dynamic performance of the system is observed.

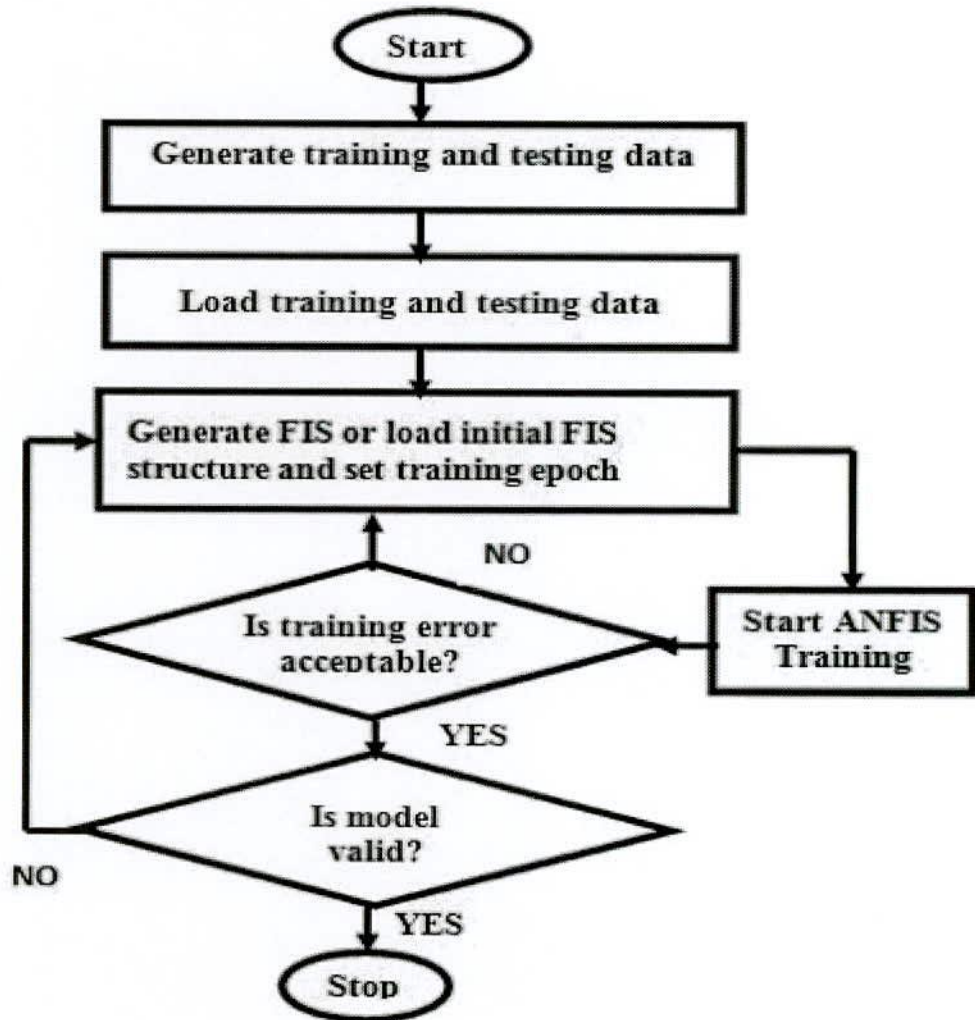


Figure 4.7: ANFIS-PSS design procedure

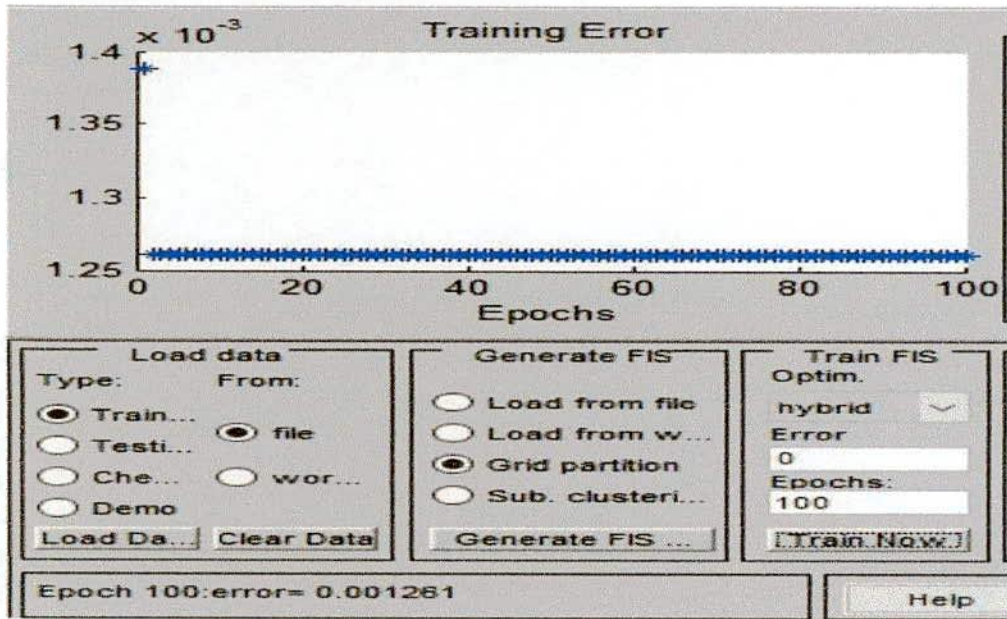


Figure 4.8: Training error of ANFIS

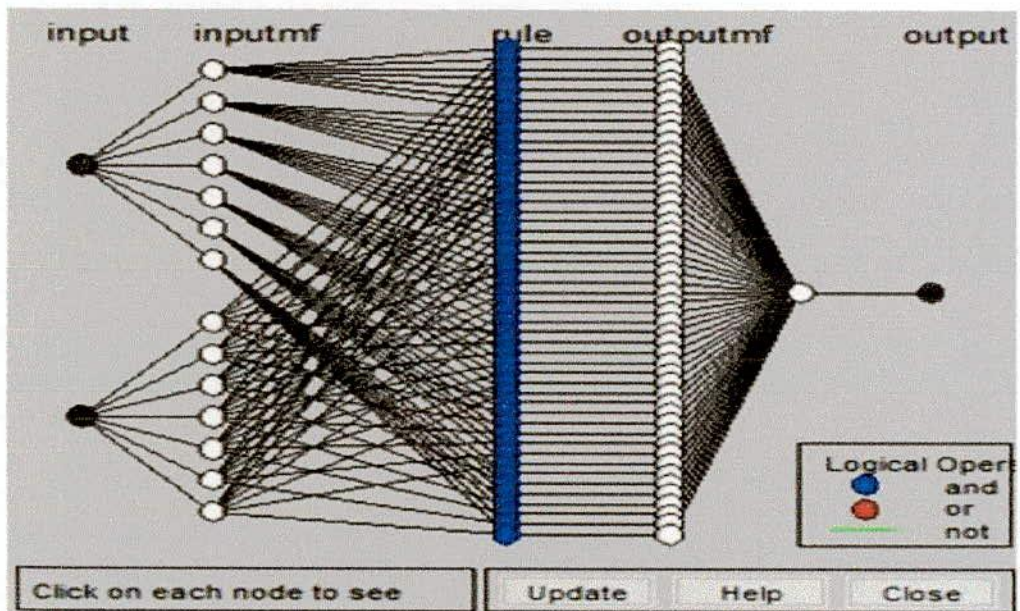


Figure 4.9: Architecture of T-S type ANFIS controller

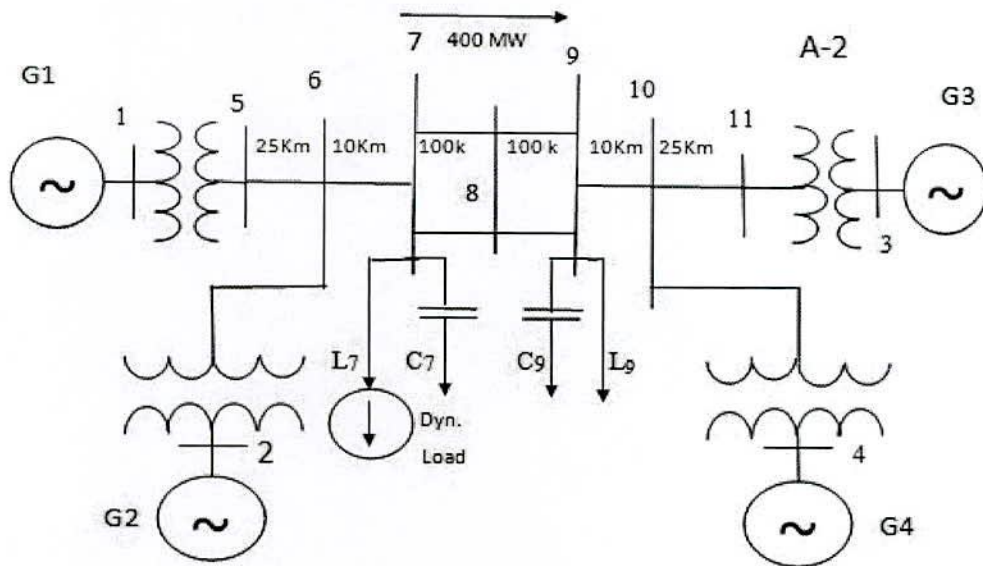


Figure 4.10: Two area network with a dynamic load

4.13 Simulation Results

The multi-machine two area complex power systems dynamic performance has been analyzed with FLC-PSS and ANFIS-based PSS. The generators are modeled by a sixth order state-space model and the dynamic load is presented by an exponential model [20] with time constants for controlling the dynamics of active and reactive power. For induction motor loads, the time constants are in the range up to one second [20]. The simulation results are described below.

- Case 1: Importance of dynamic load in power system.

Figure 4.11 shows the terminal voltage characteristics of generator 1 and generator 3 for static loads. Figure 4.12 shows the terminal voltage characteristics of generator 1 and generator 3 for dynamic loads. It is clear from the above plot that, dynamic load has huge impact on system stability. That's why load dynamics is included in this thesis.

- Case 2: performance analysis of designed PSS.

A symmetrical three phase to ground fault is applied at the middle of the transmission line, which is cleared by tipping the fault line to test the robustness of FLPSS and ANFISPSS. The simulation results can be divided into the following two parts depending on which controller is used.

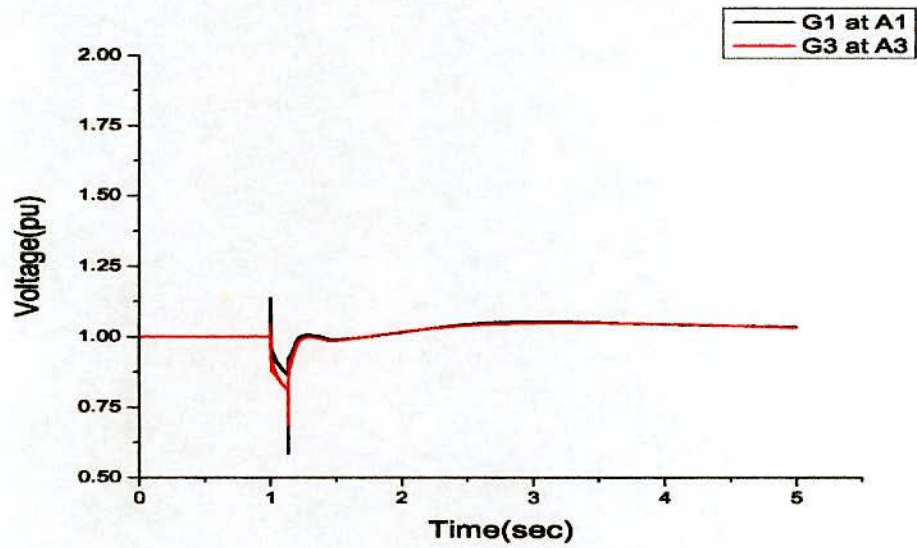


Figure 4.11: The terminal voltage characteristics of generator 1 and generator 3 for static loads.

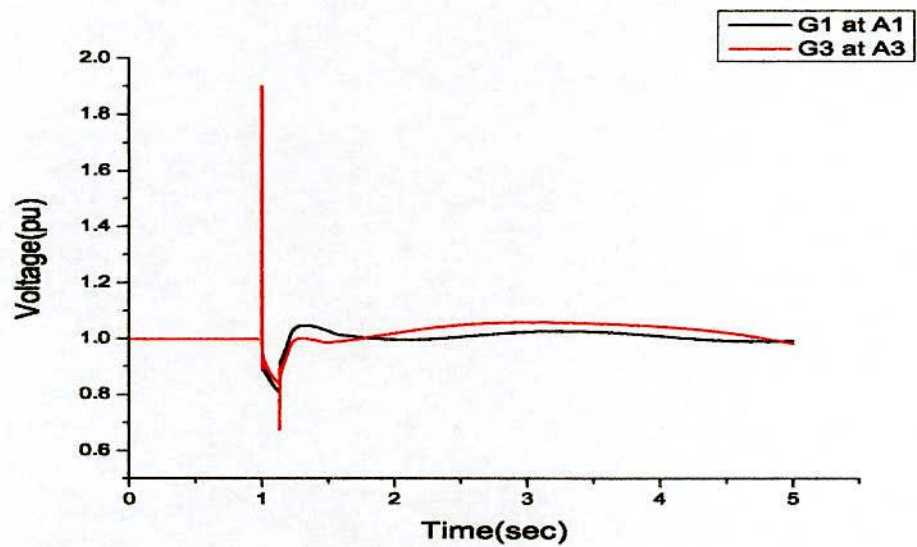


Figure 4.12: The terminal voltage characteristics of generator 1 and generator 3 for dynamic loads.

- for the FLC and.
- for the ANFIS controller.

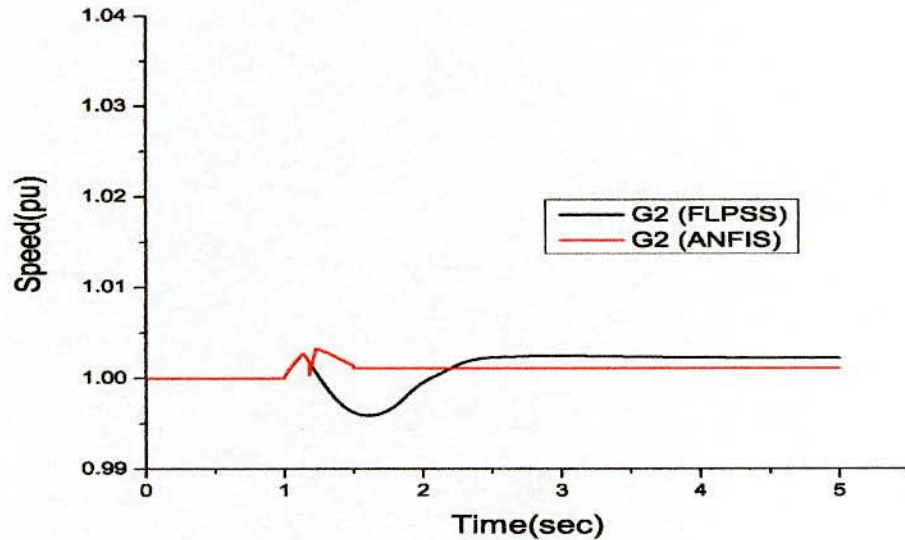


Figure 4.13: Comparative analysis of rotor speed deviation of G2 at A-1 for FLPSS and ANFIS-PSS (symmetrical three-phase fault).

Figure 4.13 shows the comparative analysis of rotor speed deviation of generator 2 at A-1 for FLPSS and ANFIS-PSS when symmetrical three-phase fault is occurred. The rotor speed deviation is significantly large for FLPSS with respect to ANFIS-PSS. Figure 4.14 shows the performance of the terminal voltage (vt) of generator 1 and generator 3 between FLPSS and ANFIS-PSS under pre-fault, faulted and post-fault condition. The active power flow from A-1 to A-2 for FLPSS and ANFIS PSS is shown in Figure 4.15. Figure 4.16 shows the voltage at the terminal of dynamic load (bus7) for FLPSS and ANFIS-PSS. It can be observed that the voltage at the bus 7, where dynamic load is connected, is reached to the steady-state value quickly for ANFIS-PSS compared to FLPSS. In both cases, the system is stable. However, in case of FLPSS rotor speed change, maximum overshoot and settling time are significant, which has improved in ANFIS-PSS. Therefore, it can be concluded that an ANFIS-PSS can be effectively used for the system having dynamic loads.

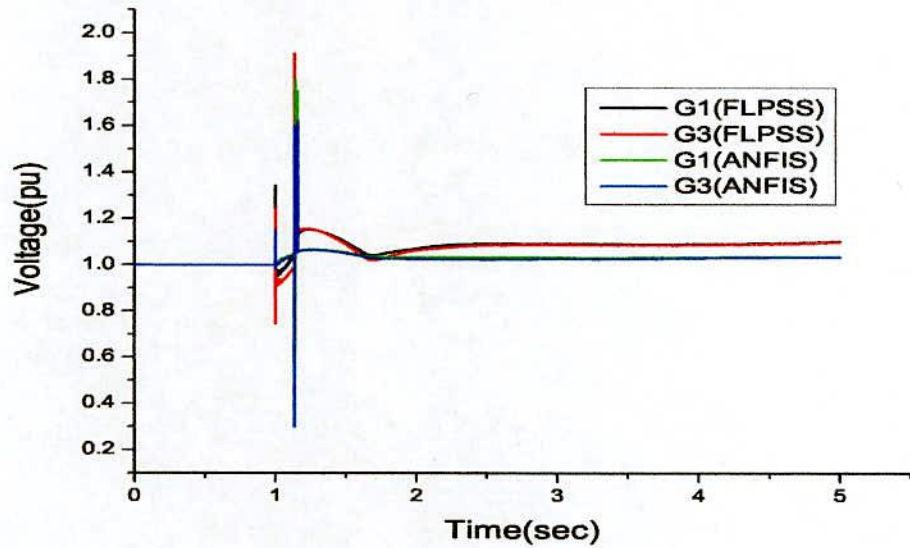


Figure 4.14: Comparative performance of terminal voltage (vt) of G1 and G3 for FLPSS and ANFIS-PSS (symmetrical three-phase fault).

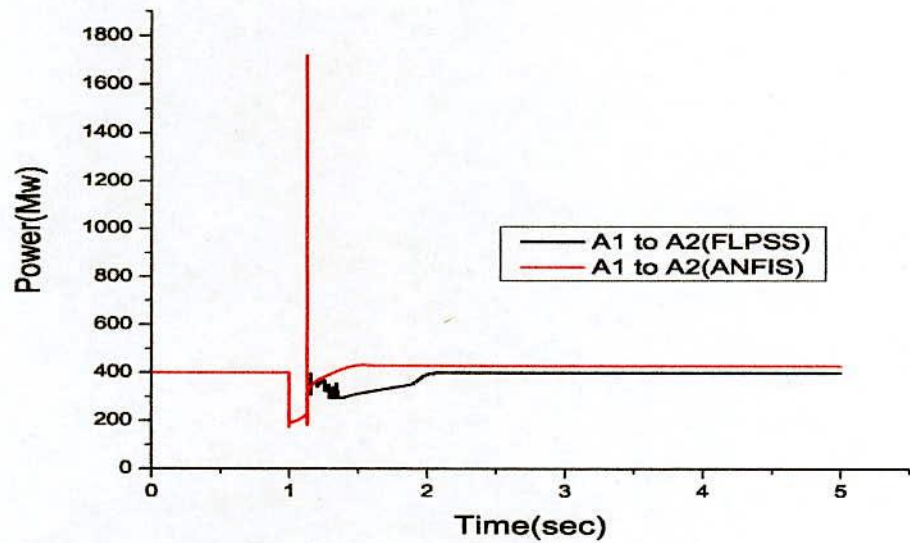


Figure 4.15: Active power flow from A-1 to A-2 for FLPSS and ANFIS PSS (symmetrical three-phase fault).

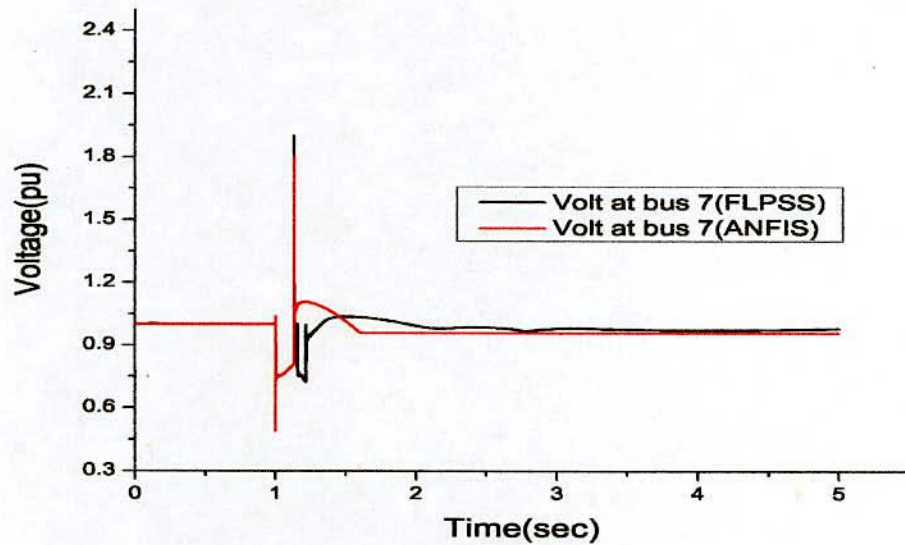


Figure 4.16: Voltage across dynamic load terminal (bus 7) for FLPSS and ANFIS-PSS (symmetrical three-phase fault).

4.14 Conclusion

In this research work, fuzzy logic and adaptive-neuro fuzzy techniques for the design of PSS are approached. The two different types of stabilizers have been tested on a two area complex multimachine system having a dynamic load under fault conditions. Simulation results illustrate the effectiveness of the proposed adaptive neuro-fuzzy based PSS specially for dynamic loads. The settling time and overshoot is minimum for ANFIS-PSS compared to FLPSS. The ANFIS-PSS shows excellent damping of low frequency electromechanical oscillation under disturbances.

Chapter 5

Selection of Best Input Signal for ANFIS-PSS

5.1 Introduction

Modern control techniques like adaptive control and H_∞ control methods have been used to achieve better performance than conventional controllers can provide. In these modern techniques, the control parameters can be adjusted quickly and continuously according to changes in demand [7]. Artificial intelligence (AI) techniques have emerged in power systems for over two decades as effective tools to solve many complex problems [49–51]. These can be even more effective when properly coupled with conventional mathematical approaches [52]. Neural network (NN) as an AI technique has efficiently been applied to power system monitoring and control. Among AI techniques (fuzzy logic and adaptive neuro-fuzzy logic) adaptive neuro-fuzzy logic are the best in terms of robustness.

5.2 Selection of best input signal

ANFIS PSS shows satisfactory performance under severe fault conditions and it is robust. However, the performance of proposed controller depends on the selection of input signals. The speed deviation and change in angular speed (angular acceleration) is used as input to ANFIS based PSS in [14, 26, 46, 53, 54]. Also, the speed deviation and power is used as input in [44]. There are many other options like accelerating power and speed deviation, speed and power, terminal voltage and power etc. can be used as input. As the issue related to the selection of input to PSS is not adequately covered in the available literature, selection of the best input for the proposed controller is carried out in this chapter.

5.3 Simulation Results

The multi-machine two area complex power systems dynamic performance has been analyzed with ANFIS-based PSS for different input signal combination. The brief description of the test system has been given in chapter 4. The simulation results can be divided into the following parts depending on the basis of input signal.

- Speed deviation and terminal voltage.
- Speed deviation and Angular Acceleration.
- Speed deviation and Accelerating power.

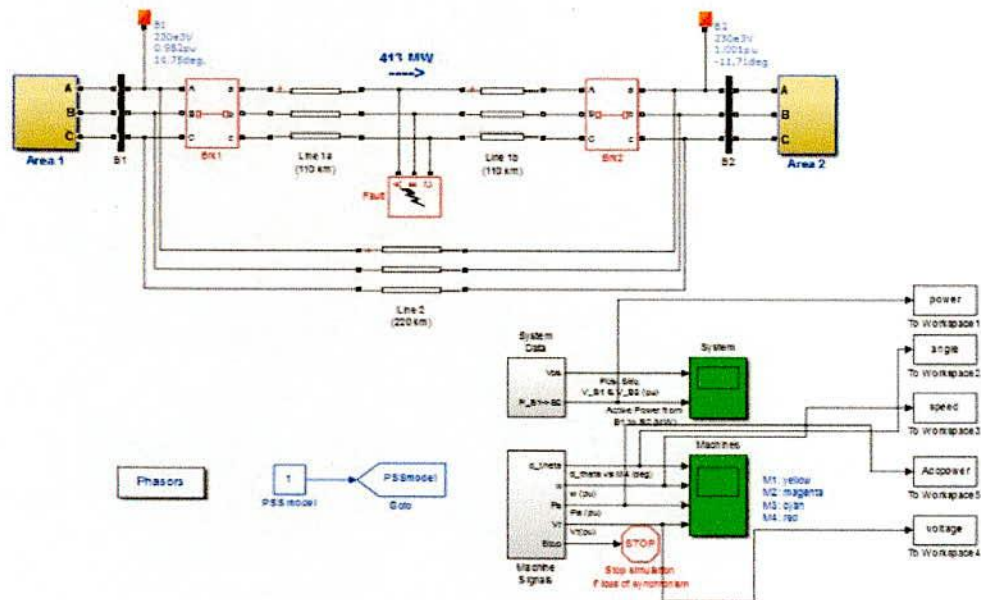


Figure 5.1: Matlab simulink model of two area test system.

Figure 5.1 shows the matlab simulink model of two area test system. Figure 5.2 shows the matlab simulink model of two area test system with ANFIS-PSS for speed deviation and voltage as input to PSS. Figure 5.3 shows the matlab simulink model of two area test system with ANFIS-PSS for speed deviation and angular acceleration as input to PSS. Figure 5.4 shows the matlab simulink model of two area test system with ANFIS-PSS for speed deviation and accelerating power as input to PSS. Transient stability analysis is more concerned with dynamic behaviors of load. To observe this a dynamic simulation is carried out.

Figure 5.5 shows the comparative analysis of rotor speed deviation of generator 3 at A-2 for three input signal combination when single line to ground fault is occurred. For speed deviation and accelerating power input signal combination performance is better. Figure 5.6 shows the comparative analysis of active power flow from A-1 to A-2 when single line to ground fault is occurred. Figure 5.7 shows the comparative performance of terminal voltage (vt) of generator 2 at A-1 when single line to ground fault is occurred. Figure 5.8 shows the comparative analysis of terminal voltage (vt) of generator 2 at A-1 when three phase to ground fault is occurred. Figure 5.9 shows the comparative analysis rotor speed deviation of generator 3 at A-2 when three phase to ground fault is occurred.

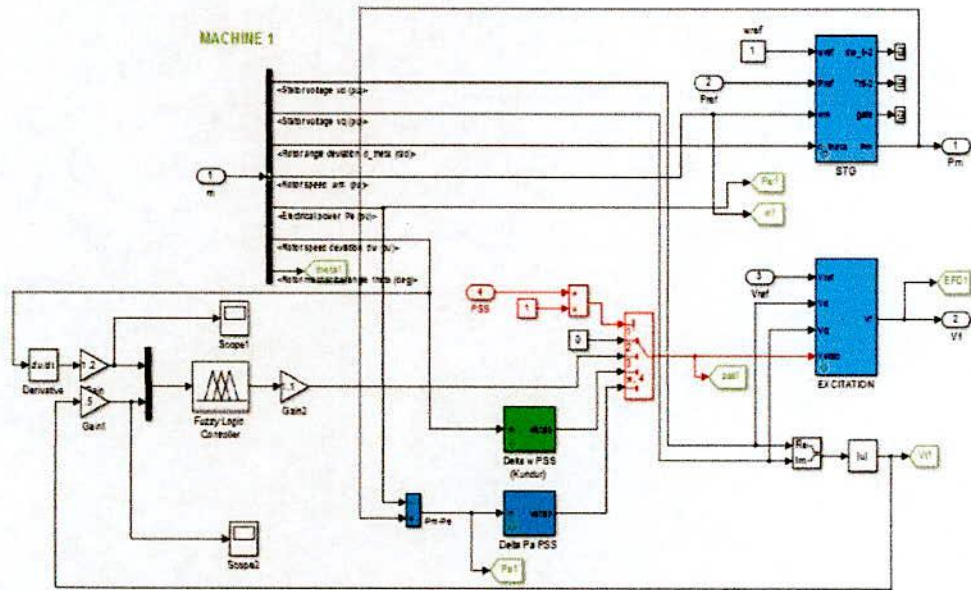


Figure 5.2: Simulink model of two area test system with ANFIS-PSS for speed deviation and voltage as input to PSS.

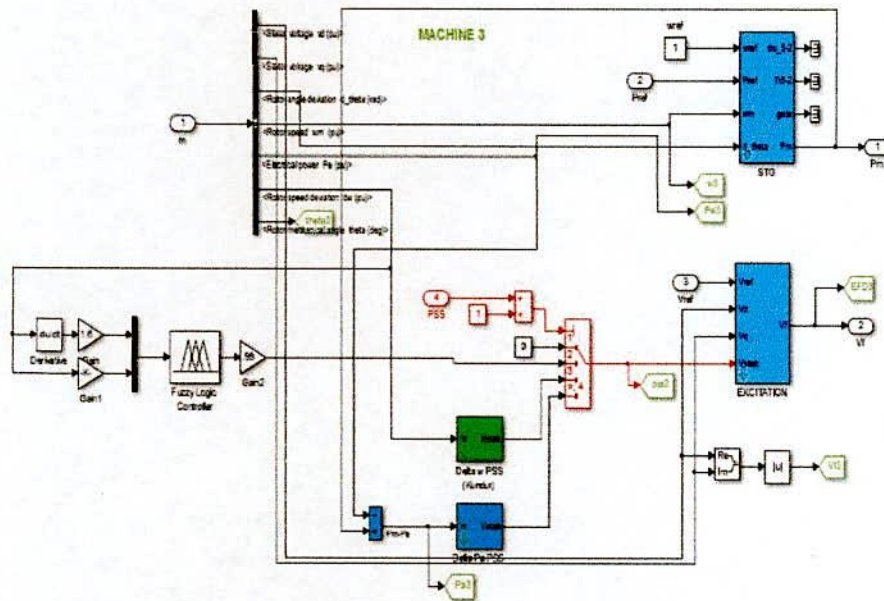


Figure 5.3: Simulink model of two area test system with ANFIS-PSS for speed deviation and angular acceleration as input to PSS.

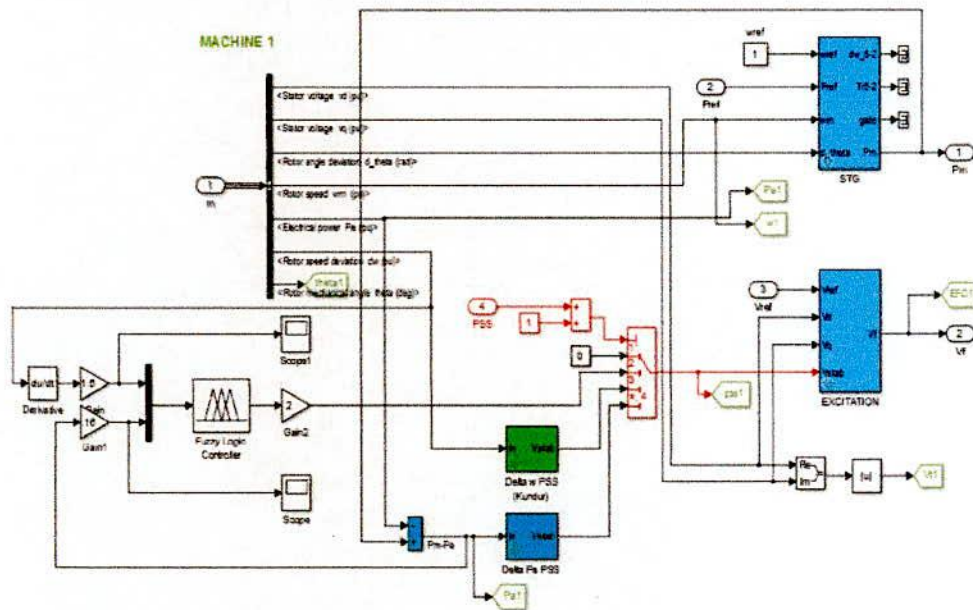


Figure 5.4: Simulink model of two area test system with ANFIS-PSS for speed deviation and accelerating power as input to PSS.

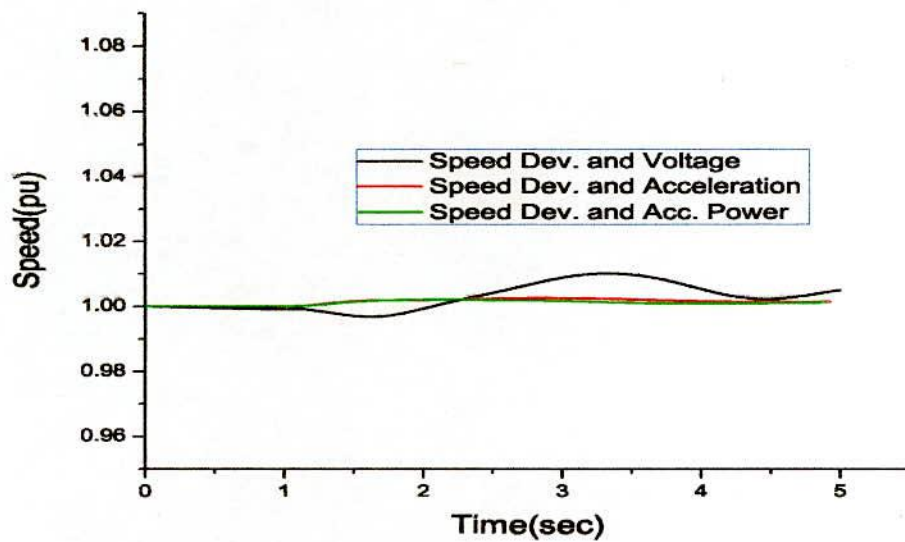


Figure 5.5: Comparative analysis of rotor speed deviation of G 3 at A-2 (single line to ground fault).

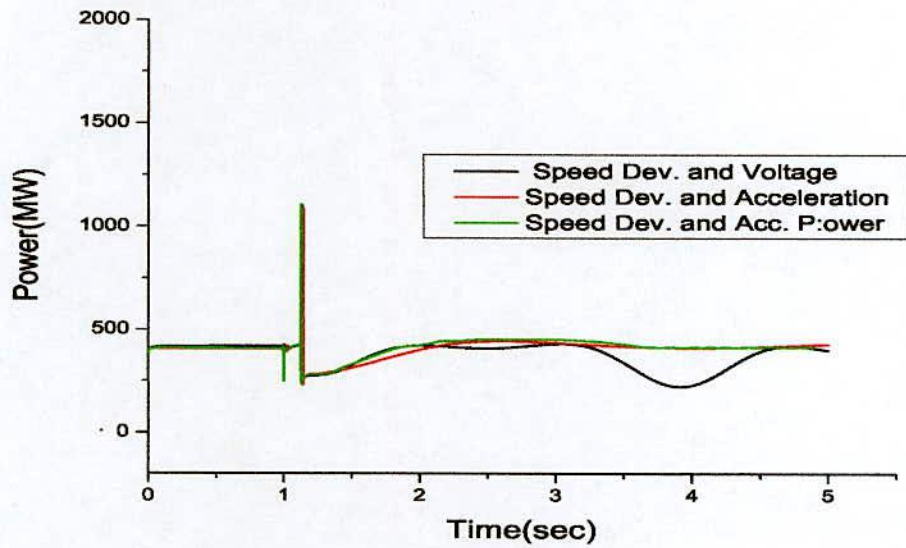


Figure 5.6: Comparative analysis of active power flow from A-1 to A-2 (single line to ground fault).

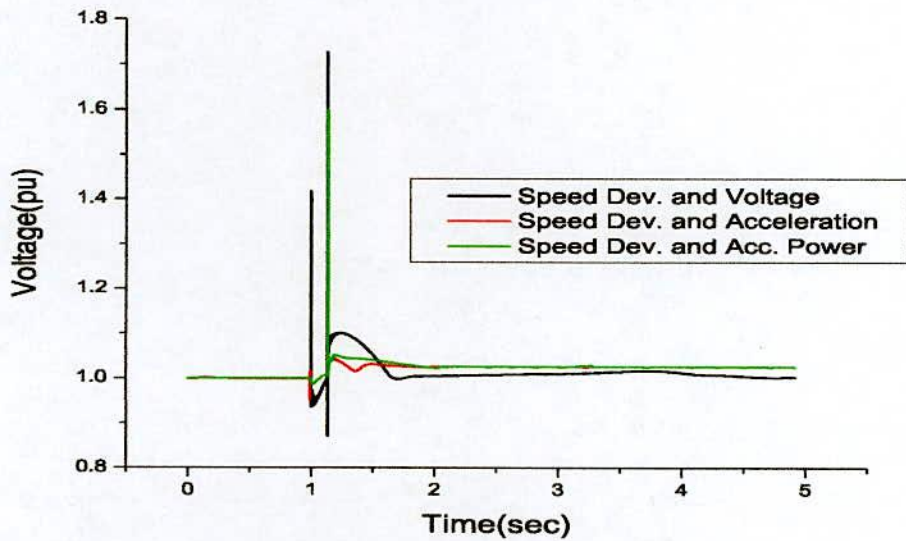


Figure 5.7: Comparative analysis of terminal voltage(vt) of G 2 at A-1 (single line to ground fault).

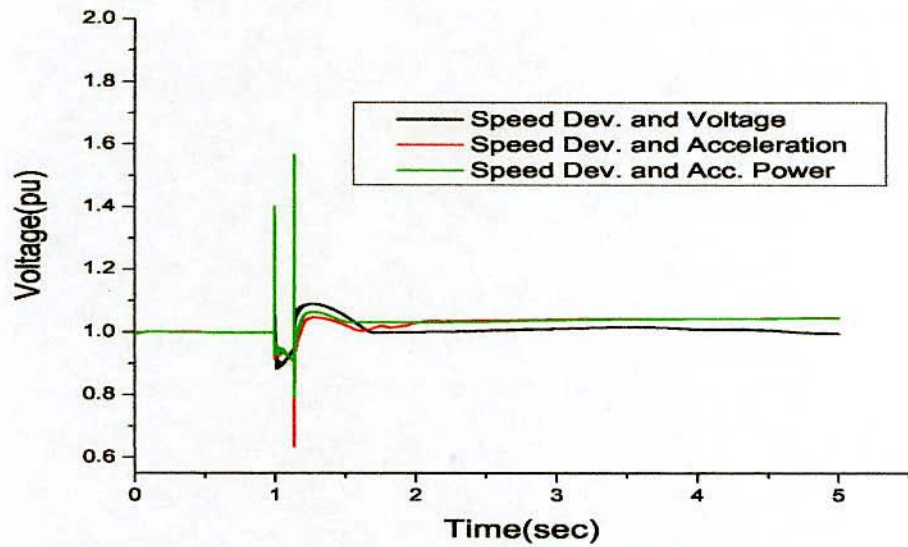


Figure 5.8: Comparative performance of terminal voltage (v_t) of G2 at A-1 (three phase to ground fault).

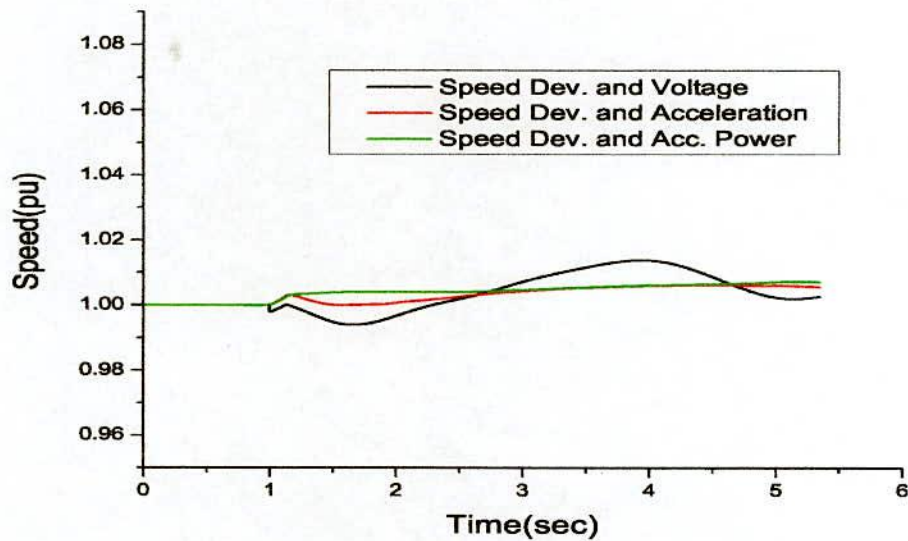


Figure 5.9: Comparative analysis of rotor speed deviation of G 3 at A-2 (three phase to ground fault).

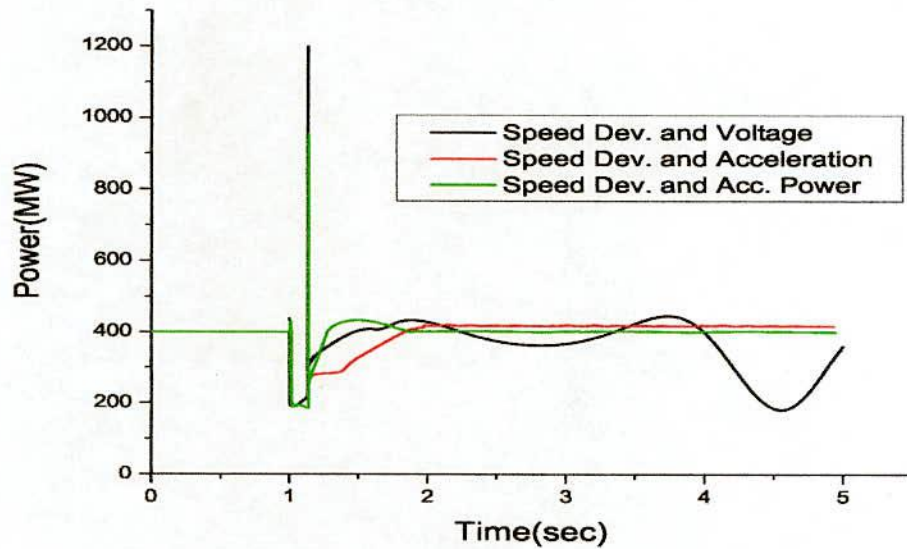


Figure 5.10: Comparative analysis of active power flow from A1 to A2 (three phase to ground fault).

Figure 5.10 Comparative analysis of active power flow from A1 to A2 when three phase to ground fault is occurred.

It is reveal that for speed deviation and accelerating power as input to ANFIS-PSS shows the best performance in all aspects. Rotor angle stability is the ability of synchronous machines of a power system to remain in synchronism. In other words, rotor angle or load angle stability denotes the angular displacement between stator and rotor speeds. It is directly proportional to the speed of the machine i.e. the load connected to the generator. If the Angle is beyond to liable limit, the system will come out of synchronism. A synchronous machine has field and armature. The field winding is energized by direct current and the rotor is driven by primeover. The rotating magnetic field of the field winding induces alternating voltages in the three phase armature winding of the stator. The frequency of the induced alternating voltages and of the resulting current that flow in the stator winding when load is connected depends on the speed of the rotor. The output power of synchronous machine varies with the rotor oscillations. In the interconnected power system, the stator voltage and current of all the machines must have the same frequency and the rotor mechanical speed of each is synchronized to this frequency. The electrical torque (power) output of the generator is changed only by changing the mechanical torque input by the primeover. The effect of increasing the mechanical torque input is to advance the rotor to a new position relative to the revolving magnetic field of the stator. Conversely, a reduction of mechanical torque or power input

will retard the rotor position. The equations of motion in per unit are

$$p\Delta\omega_r = \frac{1}{2H}(T_m - T_e - K_D\Delta\omega_r) \quad (5.1)$$

$$p\Delta\delta = \omega_0\Delta\omega_r \quad (5.2)$$

Therefore, it is wise decision to take the input signal to the feedback of the controller that comprises electrical torque, mechanical torque, speed and rotor angular position. All these things are correlated with each other. There relation is given by the above equations. Thats why for speed deviation and accelerating power as input to ANFIS-PSS shows the best performance.

5.4 Conclusion

In this chapter, transient stability is tested by applying three phase to ground fault and single line to ground fault. It is clear that speed deviation and accelerating power as input to ANFIS-PSS shows the best performance. This two input signals bear the characteristics parameters that actually affects the performance of the generators.

6.1 Conclusion

In this work, an ANFIS based power system stabilizer is designed to damp out electromechanical oscillations, which is tested on a two area test system comprising dynamic loads. Load dynamics is included because it has significant impact on power system dynamic analysis. Transient stability analysis is more concerned with dynamic behaviors of loads. The effectiveness of conventional power system stabilizer in damping oscillation is also reviewed. FLPSS shows the better control performance than conventional power system stabilizer in terms of settling time and damping effect. The rules and the membership functions parameters of the FLPSS are tuned on trial and error method. Therefore, the ANFIS-PSS is obvious as its rules and the membership functions parameters are being adjusted adaptively as well as it is more robust. The choice of input signal to the feedback path of ANFIS-PSS has an important bearing on the damping of oscillations. From the simulation studies, it shows that the oscillations are more pronounced in case of speed deviation and voltage as input to ANFIS-PSS. However, the performance of ANFIS-PSS with speed deviation and accelerating power is superior compared to other input signal combinations.

6.2 Future Research Directions

- In the present work, ANFIS-PSS has been applied as a tool to solve electromechanical oscillations problem in power system. There are a number of approaches like Linear Quadratic Gaussian (LQG), Linear Quadratic Regulator (LQR), and Genetic Algorithm that can also be applied.
- Testing using more complex network models can be carried out.
- This is simulation based study using MATLAB/SIMULINK. Testing using practical network models can be carried out.

Bibliography

- [1] Prabha Kundur, Neal J Balu, and Mark G Lauby. *Power system stability and control*, volume 7. McGraw-hill New York, 1994.
- [2] DK Sambariya and Rajendra Prasad. Robust power system stabilizer design for single machine infinite bus system with different membership functions for fuzzy logic controller. In *Intelligent Systems and Control (ISCO), 2013 7th International Conference on*, pages 13–19. IEEE, 2013.
- [3] Tomohiro Takagi and Michio Sugeno. Fuzzy identification of systems and its applications to modeling and control. *Systems, Man and Cybernetics, IEEE Transactions on*, (1):116–132, 1985.
- [4] Witold Pedrycz. *Fuzzy control and fuzzy systems (2nd*. Research Studies Press Ltd., 1993.
- [5] A Kandel. *Fuzzy expert systems*, 1992.
- [6] Prabha Kundur, John Paserba, Venkat Ajarapu, Göran Andersson, Anjan Bose, Claudio Canizares, Nikos Hatziargyriou, David Hill, Alex Stankovic, Carson Taylor, et al. Definition and classification of power system stability iee/cigre joint task force on stability terms and definitions. *Power Systems, IEEE Transactions on*, 19(3):1387–1401, 2004.
- [7] Lokman H Hassan, M Moghavvemi, Haider AF Almurib, and Otto Steinmayer. Current state of neural networks applications in power system monitoring and control. *International Journal of Electrical Power & Energy Systems*, 51:134–144, 2013.
- [8] Ashfaq A Hashmani and Istvan Erlich. Mode selective damping of power system electromechanical oscillations using supplementary remote signals. *Generation, Transmission & Distribution, IET*, 4(10):1127–1138, 2010.
- [9] Rajeev Gupta, DK Sambariya, and Reena Gunjan. Fuzzy logic based robust power system stabilizer for multi-machine power system. In *Industrial Technology, 2006. ICIT 2006. IEEE International Conference on*, pages 1037–1042. IEEE, 2006.
- [10] GY Rajaa Vikhram and S Latha. Design of power system stabilizer for power system damping improvement using optimization based linear control design. In

- Power Electronics, Drives and Energy Systems (PEDES), 2012 IEEE International Conference on*, pages 1–6. IEEE, 2012.
- [11] Prabhashankar Kundur, Meir Klein, GJ Rogers, and Malgorzata S Zywno. Application of power system stabilizers for enhancement of overall system stability. *Power Systems, IEEE Transactions on*, 4(2):614–626, 1989.
- [12] Paul M Anderson and Aziz A Fouad. *Power system control and stability*. John Wiley & Sons, 2008.
- [13] P Mitra, S Maulik, SP Chowdhury, and S Chowdhury. Anfis based automatic voltage regulator with hybrid learning algorithm. In *Universities Power Engineering Conference, 2007. UPEC 2007. 42nd International*, pages 397–401. IEEE, 2007.
- [14] PR Gandhi and SK Joshi. Ga and anfis based power system stabilizer. In *Power and Energy Society General Meeting (PES), 2013 IEEE*, pages 1–5. IEEE, 2013.
- [15] P Mitra, S Chowdhury, SP Chowdhury, SK Pal, YH Song, and GA Taylor. Damping local and inter-area oscillations with adaptive neuro-fuzzy power system stabilizer. In *Universities Power Engineering Conference, 2006. UPEC'06. Proceedings of the 41st International*, volume 2, pages 457–461. IEEE, 2006.
- [16] MA Mahmud, MJ Hossain, and HR Pota. Effects of large dynamic loads on power system stability. *International Journal of Electrical Power & Energy Systems*, 44(1):357–363, 2013.
- [17] A Rouhani and Ali Abur. Improving performance of dynamic state estimators under unknown load changes. In *Power and Energy Society General Meeting (PES), 2013 IEEE*, pages 1–5. IEEE, 2013.
- [18] A Rouhani and Ali Abur. Distributed implementation of an augmented state dynamic estimator. In *North American Power Symposium (NAPS), 2013*, pages 1–5. IEEE, 2013.
- [19] Wen-Shiow Kao, Chia-Jen Lin, Chiang-Tsang Huang, Yung-Tien Chen, and Chiew-Yann Chiou. Comparison of simulated power system dynamics applying various load models with actual recorded data. *Power Systems, IEEE Transactions on*, 9(1):248–254, 1994.
- [20] Jovica V Milanovic and IA Hiskens. Effects of load dynamics on power system damping. *Power Systems, IEEE Transactions on*, 10(2):1022–1028, 1995.
- [21] Alireza Rouhani and Ali Abur. Real-time dynamic parameter estimation for an exponential dynamic load model.
- [22] Yuan-Chyuan Lee and Chi-Jui Wu. Damping of power system oscillations with output feedback and strip eigenvalue assignment. *Power Systems, IEEE Transactions on*, 10(3):1620–1626, 1995.

- [23] Yuan-Yih Hsu and Chung-Yu Hsu. Design of a proportional-integral power system stabilizer. *Power Systems, IEEE Transactions on*, 1(2):46–52, 1986.
- [24] Ahmed Faizan Sheikh and Shelli K Starrett. Comparison of input signal choices for a fuzzy logic-based power system stabilizer. In *North American Power Symposium (NAPS), 2015*, pages 1–6. IEEE, 2015.
- [25] Ruhua You, Hassan J Eghbali, and M Hashem Nehrir. An online adaptive neuro-fuzzy power system stabilizer for multimachine systems. *Power Systems, IEEE Transactions on*, 18(1):128–135, 2003.
- [26] Jesús Fraile-Ardanuy and Pedro J Zufiria. Adaptive power system stabilizer using anfis and genetic algorithms. In *Decision and Control, 2005 and 2005 European Control Conference. CDC-ECC'05. 44th IEEE Conference on*, pages 8028–8033. IEEE, 2005.
- [27] Avdhesh Sharma and ML Kothari. Intelligent dual input power system stabilizer. *Electric Power Systems Research*, 64(3):257–267, 2003.
- [28] NK Roy, HR Pota, and TF Orchi. Small-signal stability assessment of active distribution networks with dynamic loads. In *Universities Power Engineering Conference (AUPEC), 2012 22nd Australasian*, pages 1–7. IEEE, 2012.
- [29] NK Roy, Hemanshu R Pota, A Mahmud, and Md Jahangir Hossain. D-statcom control in distribution networks with composite loads to ensure grid code compatible performance of photovoltaic generators. In *Industrial Electronics and Applications (ICIEA), 2013 8th IEEE Conference on*, pages 55–60. IEEE, 2013.
- [30] Charles P Steinmetz. Power control and stability of electric generating stations. *American Institute of Electrical Engineers, Transactions of the*, 39(2):1215–1287, 1920.
- [31] Thierry Van Cutsem and Costas Vournas. *Voltage stability of electric power systems*, volume 441. Springer Science & Business Media, 1998.
- [32] Thierry Van Cutsem. Voltage instability: phenomena, countermeasures, and analysis methods. *Proceedings of the IEEE*, 88(2):208–227, 2000.
- [33] GK Morison, B Gao, and P Kundur. Voltage stability analysis using static and dynamic approaches. *Power Systems, IEEE Transactions on*, 8(3):1159–1171, 1993.
- [34] Mathworks Documentation Center. Simpowersystems. function power_lineparam.© 1994-2014 the mathworks, inc.
- [35] PW Sauer and MA Pai. Power system dynamics and stability, prentice-hall. *New Jersey*, 1998.

- [36] Yinhong Li, Hsiao-Dong Chiang, Byoung-Kon Choi, Yung-Tien Chen, Der-Hua Huang, and Mark G Lauby. Load models for modeling dynamic behaviors of reactive loads: evaluation and comparison. *International Journal of Electrical Power & Energy Systems*, 30(9):497–503, 2008.
- [37] Les Pereira, Dmitry Kosterev, Peter Mackin, Donald Davies, John Undrill, and Wenchun Zhu. An interim dynamic induction motor model for stability studies in the wsc. *Power Systems, IEEE Transactions on*, 17(4):1108–1115, 2002.
- [38] MA Mahmud, Md Jahangir Hossain, Hemanshu R Pota, and NK Roy. Robust non-linear controller design for three-phase grid-connected photovoltaic systems under structured uncertainties. *Power Delivery, IEEE Transactions on*, 29(3):1221–1230, 2014.
- [39] Hadi Saadat. *Power system analysis*. WCB/McGraw-Hill, 1999.
- [40] Jahangir Hossain, Apel Mahmud, Naruttam K Roy, and Hemanshu R Pota. Enhancement of transient stability limit and voltage regulation with dynamic loads using robust excitation control. *International Journal of Emerging Electric Power Systems*, 14(6):561–570, 2013.
- [41] Hui Ni, Gerald Thomas Heydt, and Lamine Mili. Power system stability agents using robust wide area control. *Power Systems, IEEE Transactions on*, 17(4):1123–1131, 2002.
- [42] Ashwini Sree Venugopal, Ghadir Radman, and Mohamed Abdelrahman. An adaptive neuro fuzzy power system stabilizer for damping inter-area oscillations in power systems. In *System Theory, 2004. Proceedings of the Thirty-Sixth Southeastern Symposium on*, pages 41–44. IEEE, 2004.
- [43] Vivek Kumar Bhatt and Dr Sandeep Bhongade. Design of pid controller in automatic voltage regulator (avr) system using pso technique. *International Journal of Engineering Research and Applications (IJERA)*, 3(4):1480–1485, 2013.
- [44] AK Swagat Ranjan Swain. *Design of Power System Stabilizer*. PhD thesis, National Institute of Technology, Rourkela, 2012.
- [45] Joe H Chow, George E Boukarim, and Alexander Murdoch. Power system stabilizers as undergraduate control design projects. *Power Systems, IEEE Transactions on*, 19(1):144–151, 2004.
- [46] Neeraj Gupta. *Fuzzy logic based power system stabilizer*. PhD thesis, THAPAR UNIVERSITY PATIALA, 2008.
- [47] MF Othman, M Mahfouf, and DA Linkens. Designing power system stabilizer for multimachine power system using neuro-fuzzy algorithm. *jurnal Teknologi*, 35(1):55–64, 2012.

- [48] Kamalesh Chandra Rout. *Dynamic Stability Enhancement of Power System Using Fuzzy Logic Based Power System Stabilizer*. PhD thesis, 2011.
- [49] Lokman H Hassan and HAF Mohamed. Takagi-sugeno fuzzy gains scheduled pi controller for enhancement of power system stability. *American Journal of Applied Sciences*, 7(1):145–152, 2010.
- [50] Lokman H Hassan, Haider AF Mohamed, M Moghavvemi, and SS Yang. Load frequency control of power systems with sugeno fuzzy gain scheduling pid controller. In *ICCAS-SICE, 2009*, pages 614–618. IEEE, 2009.
- [51] Karim Sebaa and Mohamed Boudour. Optimal locations and tuning of robust power system stabilizer using genetic algorithms. *Electric Power Systems Research*, 79(2):406–416, 2009.
- [52] Mohammed E El-Hawary. *Electric power applications of fuzzy systems*. Wiley-IEEE Press, 1998.
- [53] Riad B Chedid, Sami H Karaki, and Chadi El-Chamali. Adaptive fuzzy control for wind-diesel weak power systems. *Energy Conversion, IEEE Transactions on*, 15(1):71–78, 2000.
- [54] Hossam EA Talaat, Adel Abdennour, and Abdulaziz A Al-Sulaiman. Design and experimental investigation of a decentralized ga-optimized neuro-fuzzy power system stabilizer. *International Journal of Electrical Power & Energy Systems*, 32(7):751–759, 2010.

Appendix A

The Power System Model

The state equations are:

$$\Delta \dot{x} = A\Delta x + B\Delta u$$

$$\Delta y = C\Delta x$$

Where, state variables, $x = \begin{bmatrix} \delta \\ \omega \\ E'_q \\ \Psi_d \\ E'_d \\ \Psi_q \\ V_r \end{bmatrix}$

Output variables, $y = \begin{bmatrix} V_{term} \\ \omega \\ p_e \end{bmatrix}$

Input variable, $u = V_{ref}$

$\omega =$ Angular frequency in radian/sec

$\delta =$ Rotor angle in radian

$\Psi_d, E_d =$ direct axis flux and field

$V_{term} =$ Terminal voltage

$p_e =$ Power delivered to the infinite bus

$$A = \begin{bmatrix} 0.377 & 0 & 0 & 0 & 0 & 0 & 0 \\ -0.246 & -0.156 & -0.137 & -0.123 & -0.124 & -0.0546 & 0 \\ 0.109 & 0.262 & -2.17 & 2.30 & -0.0171 & -0.0753 & 1.27 \\ -4.58 & 0 & 30 & -34.30 & 0 & 0 & 0 \\ -1.61 & 0 & 0 & 0 & -8.44 & 6.33 & 0 \\ -1.70 & 0 & 0 & 0 & 15.2 & -21.5 & 0 \\ -33.9 & -23.1 & 6.86 & -59.5 & 1.50 & 6.63 & -114 \end{bmatrix}$$

$$B = \begin{bmatrix} 0 \\ 0 \\ 0 \\ 0 \\ 0 \\ 0 \\ 16.4 \end{bmatrix}$$

$$C = \begin{bmatrix} -.123 & 1.05 & 0.23 & .207 & -.105 & -.46 & 0 \\ 0 & 1 & 0 & 0 & 0 & 0 & 0 \\ 1.42 & .9 & .787 & .708 & .713 & 314 & 0 \end{bmatrix}$$

$$D = \begin{bmatrix} 0 \\ 0 \\ 0 \end{bmatrix}$$

$$A_{33} = \begin{bmatrix} -2.17 & 2.30 & -.0171 & -.0753 & 1.27 \\ 30 & -34.3 & 0 & 0 & 0 \\ 0 & 0 & -8.44 & 6.33 & 0 \\ 0 & 0 & 15.2 & -21.5 & 0 \\ 6.86 & -59.5 & 1.5 & 6.63 & -114 \end{bmatrix}$$

$$a_{32} = \begin{bmatrix} 0.262 \\ 0 \\ 0 \\ 0 \\ -23.1 \end{bmatrix}$$

$$A_{23} = \begin{bmatrix} -0.137 & -0.123 & -0.0124 & -0.0546 & 0 \end{bmatrix}$$

K-constants are

$$K_1 = 0.0736, K_2 = 0.8644,$$

$$K_3 = 0.0331, K_4 = 1.4149,$$

$$K_5 = -.1463, K_6 = 0.4146$$

Synchronous Generator Parameters : G1 to G4

Nominal power = 900e6VA

Line to line voltage = 230e3V

Frequency=60Hz

The d-axis Synchronous reactance, $X_d = 1.8\text{pu}$

The d-axis transient reactance, $X'_d = 0.3\text{pu}$

The d-axis subtransient reactance, $X''_d = 0.25\text{pu}$

The q-axis synchronous reactance, $X_q = 1.7\text{pu}$

The q-axis transient reactance, $X'_q = 0.55\text{pu}$

The q-axis subtransient reactance, $X''_q = 0.25\text{pu}$

The d-axis transient open-circuit time constant, $(T_{do'}) = 8\text{s}$

The d-axis subtransient open-circuit time constant, $(T''_{do}) = 0.03\text{s}$

The q-axis transient open-circuit time constant, $(T'_{qo}) = 0.4\text{s}$

The q-axis subtransient open-circuit time constant, $(T''_{qo}) = 0.05\text{s}$

Leakage reactance, $X_l = 0.2\text{pu}$

Inertia constant, $H(\text{s}) = 6.5\text{s}$ for G1 and G2

Inertia constant, $H(\text{s}) = 6.175\text{s}$ for G3 and G4

Line Parameters

The parameters of the lines in pu unit on 100MVA, 230KV base are

$$r=0.0001\text{pu/km}$$

$$x_l = 0.001\text{pu/km}$$

$$b_c = 0.00175\text{pu/km}$$

Transformer Parameters

Nominal power = 900e6VA

Frequency=60Hz

Winding 1 parameters

$$v_1(\text{rms}) = 20\text{e}3\text{V}(ph - ph)$$

$$r_1 = 1\text{e} - 6\text{pu}$$

$$L_1 = 0\text{pu}$$

Winding 2 parameters

$$v_2(\text{rms}) = 230\text{e}3\text{V}(ph - ph)$$

$$r_2 = 1\text{e} - 6\text{pu}$$

$$L_2 = 0\text{pu}$$

Magnetization resistance, $R_m = 500$ pu

Magnetization inductance, $L_m = 500$ pu

Dynamic Load Parameters:

Nominal line to line voltage $V_n(V_{rms})=230\text{e}3\text{V}$

Frequency=60Hz

Active power(P_0)= 967e6VA

Reactive Power, (Q_0)=100e6Var

Exponents, $np = 1.3$ & $nq = 2$

Time constants, $T_{p1}=0.1$

$$T_{p2} = 0.1$$

$$T_{q1} = 0.1$$

$$T_{q2} = 0.1$$

$$V_{min} = 0.7\text{pu}$$

Initial positive sequence voltage, $V_0=0.994\text{pu}$

Publications List

1. **Moudud Ahmed** and Naruttam Kumar Roy, "Design of a Power System Stabilizer Using Adaptive Neuro-Fuzzy Logic for a Multi-Machine System Having Dynamic Loads," In the 5th International Conference on Informatics, Electronics & Vision (ICIEV), May, 2016, Dhaka, Bangladesh.
2. **Moudud Ahmed** and Naruttam Kumar Roy, "A Comparative Analysis on Different Types of Power System Stabilizers," In the 5th International Conference on Informatics, Electronics & Vision (ICIEV), May, 2016, Dhaka, Bangladesh.
3. **Moudud Ahmed** and Naruttam Kumar Roy, "Selection of Best Input Signals to ANFIS-Based Power System Stabilizers for Multi-Machine Power Systems," International Journal of Electrical Power & Energy Systems (ELSEVIER), Impact Factor 2.193, Submitted, May, 2016.